



BSI Standards Publication

**Railway applications —
Acoustics — Measurement
method for combined
roughness, track decay rates
and transfer functions**

National foreword

This Published Document is the UK implementation of CEN/TR 16891:2016.

The UK participation in its preparation was entrusted by Technical Committee EH/1, Acoustics, to Subcommittee EH/1/2, Transport noise.

A list of organizations represented on this committee can be obtained on request to its secretary.

This publication does not purport to include all the necessary provisions of a contract. Users are responsible for its correct application.

© The British Standards Institution 2016.

Published by BSI Standards Limited 2016

ISBN 978 0 580 74370 2

ICS 17.140.30; 93.100

Compliance with a British Standard cannot confer immunity from legal obligations.

This British Standard was published under the authority of the Standards Policy and Strategy Committee on 30 June 2016.

Amendments/corrigenda issued since publication

Date	Text affected
-------------	----------------------

TECHNICAL REPORT

CEN/TR 16891

RAPPORT TECHNIQUE

TECHNISCHER BERICHT

May 2016

ICS 17.140.30; 93.100

English Version

Railway applications - Acoustics - Measurement method for combined roughness, track decay rates and transfer functions

Bahnanwendungen - Akustik - Messmethode für
kombinierte Rauheit, Gleisabklingraten und
Übertragungsfunktionen

This Technical Report was approved by CEN on 13 May 2016. It has been drawn up by the Technical Committee CEN/TC 256.

CEN members are the national standards bodies of Austria, Belgium, Bulgaria, Croatia, Cyprus, Czech Republic, Denmark, Estonia, Finland, Former Yugoslav Republic of Macedonia, France, Germany, Greece, Hungary, Iceland, Ireland, Italy, Latvia, Lithuania, Luxembourg, Malta, Netherlands, Norway, Poland, Portugal, Romania, Slovakia, Slovenia, Spain, Sweden, Switzerland, Turkey and United Kingdom.



EUROPEAN COMMITTEE FOR STANDARDIZATION
COMITÉ EUROPÉEN DE NORMALISATION
EUROPÄISCHES KOMITEE FÜR NORMUNG

CEN-CENELEC Management Centre: Avenue Marnix 17, B-1000 Brussels

Contents		Page
European foreword		4
Introduction		5
1	Scope	6
2	Normative references	6
3	Terms and definitions	7
4	Symbols and abbreviations	8
5	Instrumentation	8
6	Installation aspects	9
7	Measurement positions	9
8	Measured quantities	10
9	Test procedure	10
10	Data processing	10
11	Method to determine the track decay rate from rail vibration	11
11.1	General	11
11.2	Energy iteration method	11
12	Method to determine the combined roughness from vertical railhead vibration	18
13	Method to convert roughness from frequency to wavelength domain	20
14	Method to determine the rolling noise transfer function	22
14.1	Definition	22
14.2	Application examples	23
15	Test report	23
16	Uncertainty and grade	23
Annex A (informative) A₂ factor, difference between the combined roughness and the contact point displacement		25
Annex B (informative) Benchmark examples and background information		28
B.1	General	28
B.2	Examples of vertical decay rates determined for several different tracks	28
B.3	Comparison with direct measurements	29
B.4	Comparison of TDR methods	33
B.5	Repeatability	35
B.6	Reproducibility	38
B.7	Effect of accelerometer position	42
B.8	Effect of speed and averaging	48
B.9	Effect of wheel defects	52

B.10	Effect of temperature	52
B.11	Effect of load	52
Annex C (informative)	Slope methods.....	53
C.1	Single accelerometer slope method.....	53
C.2	Two accelerometer method.....	54
Bibliography	55

European foreword

This document (CEN/TR 16891:2016) has been prepared by Technical Committee CEN/TC 256 "Railway applications", the secretariat of which is held by DIN.

Attention is drawn to the possibility that some of the elements of this document may be the subject of patent rights. CEN shall not be held responsible for identifying any or all such patent rights.

Introduction

This Technical Report provides a basis for a standard on measurement of combined wheel-rail roughness, track decay rates and transfer functions from train pass-bys.

The main items required for a standard are covered but also additional background information and benchmark results are included.

1 Scope

This method is used to determine combined wheel-rail roughness and track decay rates from rail vibration during the pass-by of a train. By combining sound pressure measurement from the same pass-by, a vibro-acoustic transfer function for rolling noise is determined.

The track decay rate is a vibration quantity that characterizes the attenuation of rail vibration along the track for a given wheel/rail contact excitation, and thereby affects the amount of sound radiation from the track.

Combined roughness is a quantity that determines the level of excitation of wheel-rail rolling noise. It can be determined from vertical rail vibration during a train pass-by and the vertical track decay rate. The transfer function can be used to characterize the vibro-acoustic behaviour of the vehicle-track system for a given roughness excitation and in relation to rolling noise. Combined roughness, track decay rates and transfer functions are determined as one-third octave spectra.

The method can be used for the following purposes:

- to measure track decay rates under operational conditions;
- to characterize the effectiveness of noise control measures in terms of combined roughness, transfer function and track decay rate;
- to compare the combined roughness before and after noise control measures are implemented (thereby quantifying the effect of any change in wheel or rail roughness);
- to monitor wheel roughness during a pass-by, either of whole trains or parts of trains;
- to separate rolling noise from other sources;
- to assess a threshold for the rail roughness by measuring multiple pass-bys.

The method is not for approval of sections of reference track in terms of acoustic rail roughness and track decay rates, which are covered by EN 15610 and EN 15461, respectively.

The method is applicable to trains on conventional tracks, i.e. normal ballasted tracks with wooden or concrete sleepers and on ballastless track systems.

The method has not yet been validated for:

- non-standard wheel types such as small wheels up to 600 mm diameter, resilient tram wheels;
- non-standard track types such as embedded rail or grooved rail;

The method is not applicable to track with rail joints.

2 Normative references

The following documents, in whole or in part, are normatively referenced in this document and are indispensable for its application. For dated references, only the edition cited applies. For undated references, the latest edition of the referenced document (including any amendments) applies.

EN 15461, *Railway applications — Noise emission — Characterisation of the dynamic properties of track sections for pass by noise measurements*

EN 15610, *Railway applications — Noise emission — Rail roughness measurement related to rolling noise generation*

EN ISO 266, *Acoustics — Preferred frequencies (ISO 266)*

3 Terms and definitions

For the purposes of this document, the following terms and definitions apply.

3.1

pass-by time

t_p [s]

duration of vehicle pass-by from buffer to buffer

3.2

number of axles

N_{ax} [-]

number of axles in the selected train or part of train

3.3

one-third octave band frequency

f_c [Hz]

centre frequency of a one-third octave frequency band

3.4

one-third octave wavelength

λ [m]

centre wavelength of a one-third octave wavelength band

3.5

sound pressure signal

$p(t)$ [Pa]

time signal of the sound pressure measured at a fixed point

3.6

equivalent sound pressure level spectrum

$L_{peq, T_p}(f_c)$ dB re $2 \cdot 10^{-5}$ [Pa]

one-third octave spectrum of the sound pressure energy averaged over pass-by time t_p

3.7

acceleration signal

$a(t)$ [m/s^2]

time signal of the rail acceleration

3.8

equivalent vertical rail vibration level spectrum

$L_{aeq, T_p}(f_c, v)$ dB re 10^{-6} [m/s^2]

one-third octave spectrum of the sound pressure energy averaged over pass-by time t_p at running speed v

3.9

decay exponent

β [m^{-1}]

decay exponent characteristic for the vibration decay in the rail

3.10
vertical track decay rate
 $D_z(f_c)$ [dB/m]

decay rate of vertical rail vibrations along the rail head

3.11
lateral track decay rate
 $D_y(f_c)$ [dB/m]

decay rate of lateral rail vibrations along the rail head

3.12
combined effective roughness wavelength spectrum
 $L_{Rtot}(\lambda)$, dB re 10^{-6} [m]

wavelength spectrum in one-third octaves of the combined effective wheel-rail roughness including the contact filter

3.13
combined effective roughness frequency spectrum at speed v
 $L_{Rtot}(f_c, v)$ dB re 10^{-6} [m]

frequency spectrum in one-third octaves of the combined effective wheel-rail roughness including the contact filter

3.14
rolling noise transfer function
 $L_{HpR,tot,nl}(f_c)$ [dB re 20 Pa/ \sqrt{m}]

transfer function in one-third octave bands between the sound pressure at a fixed point, 7,5 m, and the combined effective roughness frequency spectrum, normalized to the axle density N_{ax}/l

4 Symbols and abbreviations

Symbol	Definition	Unit
l	length of train, vehicle or train part	[m]
v	train speed	[m/s]

5 Instrumentation

Instrumentation for sound pressure measurement should comply with requirements in EN ISO 3095.

The whole measurement chain shall be capable of measuring in the frequency range 25 Hz to 10 kHz. The signal sample rate for acceleration and sound pressure signals should be sufficient for the frequency range required. A sample frequency of 25 kHz or 32 kHz is sufficient for a measurement range up to 10 kHz.

The accelerometer type should be consistent with the expected vibration range and frequency range. The accelerometer and its measurement chain shall be selected and adjusted to cover the typical vibration range without signal clipping or overloading. Vertical railhead vibration can reach up to 5 000 m/s^2 or more. The dynamic range shall be at least 70 dB.

The accelerometer and its connector shall be water tight especially if moisture can collect during the measurement.

Optionally a thermometer should be available for measuring the rail temperature.

6 Installation aspects

The accelerometer should be fixed to the rail by means of a glue

NOTE Magnetic fixing is also possible but may reduce the usable frequency range at higher frequencies.

General guidelines on mechanical mounting of accelerometers should be taken into account as set out in ISO 5348.

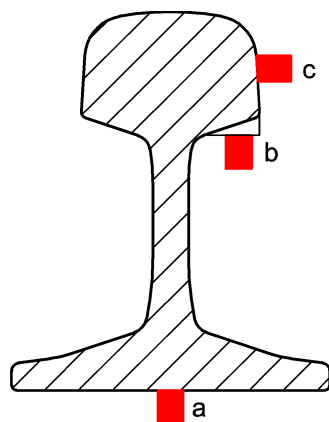
Attention should be given to firm mounting as the resonance frequency of the accelerometer on its mounting can drop below 10 kHz if not sufficiently stiff.

Overloading and potential loosening or detachment should be avoided and therefore continually monitored during measurement.

Further information on installation aspects can be found in [10].

7 Measurement positions

For vertical track decay rate and combined roughness measurement a single accelerometer is mounted under the longitudinal axis of the rail foot or under the side of the rail head (with angle plate, see Figure 1), next to a sleeper. For lateral decay rate measurement an accelerometer is mounted on the outer side of the rail head. If the transfer function is measured then a microphone is positioned at 7,5 m from the track centreline and at 1,2 m above the rail surface directly opposite the accelerometer. The number of accelerometers may be increased if required, for example to measure the combined roughness on the other rail or along the track to take potential track variations into account.



a) Cross section of the rail, wheel flange on the left side



b) Example of position a

Figure 1 — Suitable positions for measuring vertical railhead vibration a and b

Mounting underneath the side of the railhead (b) should include an angle stud to ensure vertical positioning of the accelerometer. Position c indicates the position for lateral railhead vibration measurement, if required.

The measurement cross-section shall not be close to unusual rail support conditions, in particular:

- 1) there shall be no pumping sleeper within a distance smaller than 3 m to the accelerometer;
- 2) there shall be no missing or damaged rail clip (or fastener of any other type, if necessary) on the supports directly adjacent to the accelerometer location;

- 3) the accelerometer shall not be located within 5 m of a weld;
- 4) the accelerometer shall not be located within 40 m of an expansion joint.

8 Measured quantities

- Pass-by time t_p of train or train part;
- train speed v ;
- vertical railhead acceleration signal $a(t)$;
- sound pressure signal at 7,5 m $p(t)$;
- optionally axle trigger signal $z(t)$ should be recorded during the measurements;
- optionally the rail temperature should be recorded during the measurements.

9 Test procedure

During a whole pass-by of a train the following is recorded:

- vertical railhead vibration (acceleration signal) including the approach and departure of the train;
- sound pressure time signal, if a transfer function is required;
- train speed v ;
- train length ℓ , usually determined from known vehicle lengths;
- number of axles N_{ax} counted or estimated from the vibration or trigger signal;
- optionally the axle trigger signal $z(t)$.

If the lateral decay rate is to be determined, then also lateral railhead vibration shall be registered.

The vertical track decay rate and, if required, the lateral track decay rate shall be averaged over several pass-bys of one or more trains, rejecting outlier curves, see Clause 11.

An indicative result (which shall not be considered as a valid result) of the combined roughness and transfer function can be obtained from a single pass-by.

The measurement uncertainty can be reduced by:

- averaging results over three or more pass-bys of the same train;
- averaging results over two or more train speeds of the same train at least 10 % apart.

Combined roughness can be measured either on a single rail or on both rails depending on the purpose of the measurement.

10 Data processing

The vertical (and if required lateral) rail acceleration time signal is processed by the method described in Clause 11 to determine the track decay rate.

The combined roughness is derived from the vertical decay rate and the equivalent rail vibration level $L_{aeq,tp}$ over pass-by time t_p according to the method set out below. The transfer function is derived according to Clause 14 from the equivalent sound pressure level $L_{peq}(f_c)$, the combined roughness $L_{Rtot}(f_c, v)$ and the number of axles per unit length N_{ax}/ℓ .

11 Method to determine the track decay rate from rail vibration

11.1 General

The track decay rate (both vertical and lateral) shall be determined by the energy iteration method described in 11.2. Alternative methods analysing the slope of the time signal are described in Annex C.

The slope methods described in Annex C generally do not eliminate the contributions from other wheels and can therefore give an underestimation of the decay rate. In addition, where manual interaction is required during processing, more errors can occur in selecting the location of the defining points. The energy method takes the contributions of other wheels into account and is less sensitive to manual inputs as long as the wheel positions are correctly specified. Examples of results from the slope methods compared to the energy method are given in B.3.

Results shall be averaged over at least 3 pass-bys. The average shall be the arithmetic mean of track decay rate levels in each one-third octave frequency band. Results differing by more than 5 dB in any one-third octave frequency band should be rejected, at least in the frequency range concerned.

11.2 Energy iteration method

The energy iteration method to derive the decay rate from the vibration time signal is analogous to the hammer impact method described in EN 15461, with the difference that the moving wheel provides the excitation instead of a hammer, and the track has a real load. Also the signal energy is higher than when using a hammer.

The rail vibration amplitude due to a single wheel is assumed to be described by an exponential function:

$$A(x) \approx A(0)e^{-\beta x} \quad (1)$$

Where

- x is the position away from the contact point along the rail;
- $A(x)$ is the vibration amplitude along the rail;
- $A(0)$ is the instantaneous amplitude at the position of the wheel contact point;
- β is a decay exponent.

The decay rate D_z in dB/m can be given as:

$$D_z = 20 \log_{10}(e^\beta) \approx 8,686\beta \text{ [db/m]} \quad (2)$$

This decay rate is derived from the evaluation of the ratio of the integrated vibration energy over a length L_2 , potentially including the whole train pass-by versus the integrated vibration energy over a short length L_1 directly around the wheels. L_1 is taken as the shortest axle distance in the train (or part of the train). A common minimum wheel distance is 1,8 m, in which case the analysis length L_1 extends from -0,9 m to +0,9 m around each wheel position. The wheel position is determined by a wheel trigger signal or manually from the acceleration signal. In the latter case, a sufficiently high signal sampling rate is required to accurately locate the axle positions, see Clause 8.

The integrated squared vibration over a length L_1 around all N wheels is, using Formula (1):

$$A_{\Sigma L_1}^2 = \sum_{n=1}^N A_{n,L_1}^2 = \sum_{n=1}^N \int_{-L_1/2}^{L_1/2} \left(A_n(0) e^{-\beta|x|} \right)^2 dx = \frac{1 - e^{-\beta L_1}}{\beta} \sum_{n=1}^N A_n^2(0) \quad (3)$$

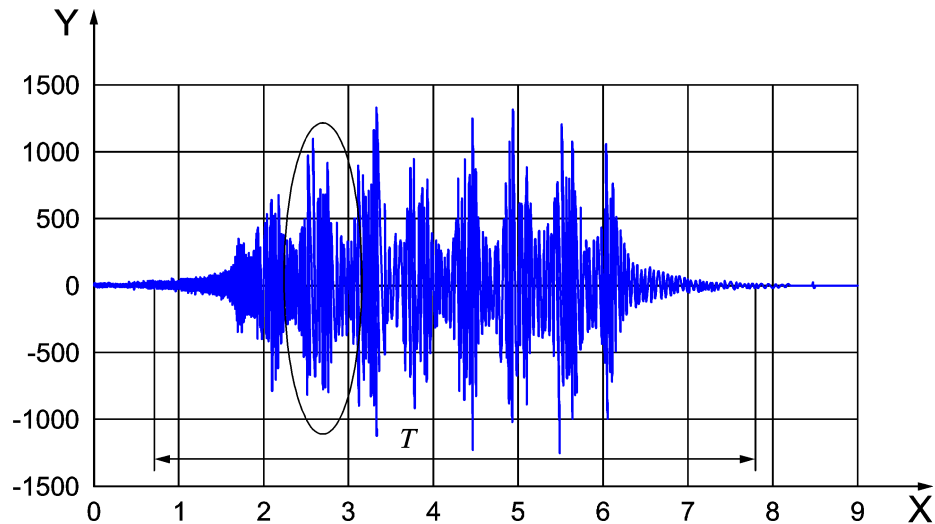
Similarly, the integrated squared vibration over a long length L_2 incorporating all N wheels is:

$$\sum_{n=1}^N \int_{L_2} \left(A_n(0) e^{-\beta|x|} \right)^2 dx = \frac{1 - e^{-\beta L_2}}{\beta} \sum_{n=1}^N A_n^2(0) \approx \frac{1}{\beta} \sum_{n=1}^N A_n^2(0) \quad (4)$$

The approximation at the right hand side in the above formula is valid for sufficiently large L_2 , e.g. a train length or the length of a (group of) vehicle(s).

The quantities $A_{\Sigma L_1}^2$ and $A_{\Sigma L_2}^2$ can be determined straightforwardly from measured acceleration signals. The transducer time signal is passed through one-third octave band pass filters resulting in a filtered time signal. Then, for each frequency band, the integrated squared vibration is determined over every wheel over length L_1 (time T_x), see Figure 2a and for the whole pass-by (whole train) for L_2 (time T). Using Formulae (3) and (4) the vibration energy ratio R of $A_{\Sigma L_1}^2$ and $A_{\Sigma L_2}^2$ for each one-third octave band frequency f_c is given as:

$$R(f_c) = \frac{A_{\Sigma L_1}^2(f_c)}{A_{\Sigma L_2}^2(f_c)} \approx 1 - e^{-\beta L_1} \quad (5)$$

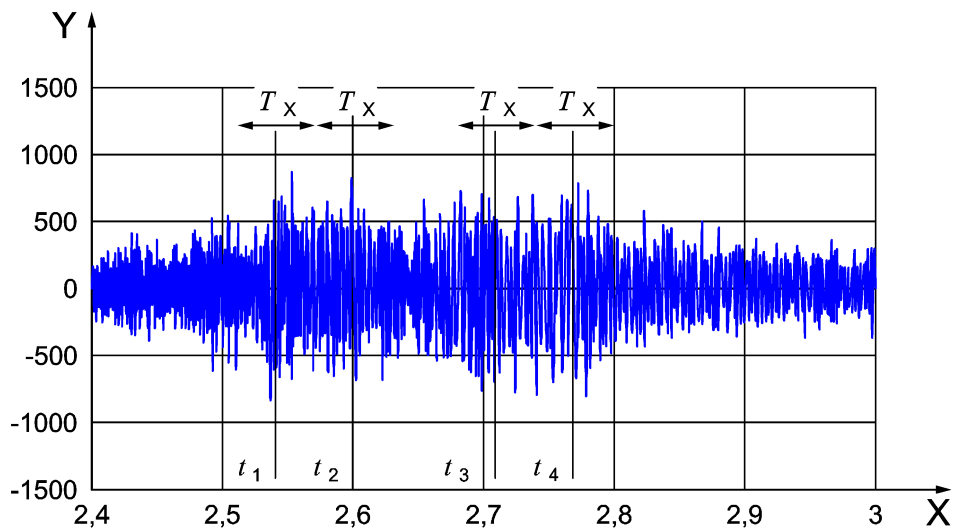


Key

Y acceleration in m/s^2

X time in s

a) Unfiltered time signal of whole pass-by with total integration time T indicated



Key

Y acceleration in m/s^2

X time in s

NOTE The integration is applied to the bandpass-filtered time signal for each one-third octave band.

b) Selected part of time signal indicated showing integration time T_x around each wheel

Figure 2 — Time signal of vertical rail vibration

The T_x interval contains mainly energy from the single wheel, but also contributions from other wheels, particularly the nearby ones. T_x should be chosen to be slightly shorter than the shortest distance between wheels over the whole train to avoid overlap in energy summation.

From Formula (5) and Formula (2) the vibration decay rate D_z (TDR) is determined from:

$$D_z(f_c) = -\frac{8,686}{L_1} \ln(1 - R(f_c)) \quad (6)$$

The measured vertical rail acceleration level potentially contains contributions from all wheels. So the pass-by slopes of the vibration level are also affected by these contributions and need to be adjusted accordingly. This can be done by the following iteration procedure illustrated in Figure 3:

- A formula for estimating the decay exponent $\beta(f_c)$ at each band frequency is based on Formula (5), similar to Formula (6). The vibration energy ratio $R(f_c)$ is determined for the whole train pass-by or selected part of it as in Formula (5), and multiplied by $N/w_k(f_c)$, where N = number of axles and $w_k(f_c)$ = weighting coefficient.

$$\beta_k(f_c) = -\frac{\ln\left(1 - \frac{R(f_c)N}{w_k(f_c)}\right)}{L_1} \quad (7)$$

A starting estimate for the initial decay exponent $\beta_1(f_c)$ is obtained with $w_1 = 2 N$. This initial condition $w_1 = 2 N$ assumes that half the vibration energy at each wheel is from other wheels.

- The subsequent iterations are then calculated until the decay exponent $\beta_i(f_c)$ is stable to within 0,5 dB, which is often achieved after four iteration steps $k = 2$ to 5:

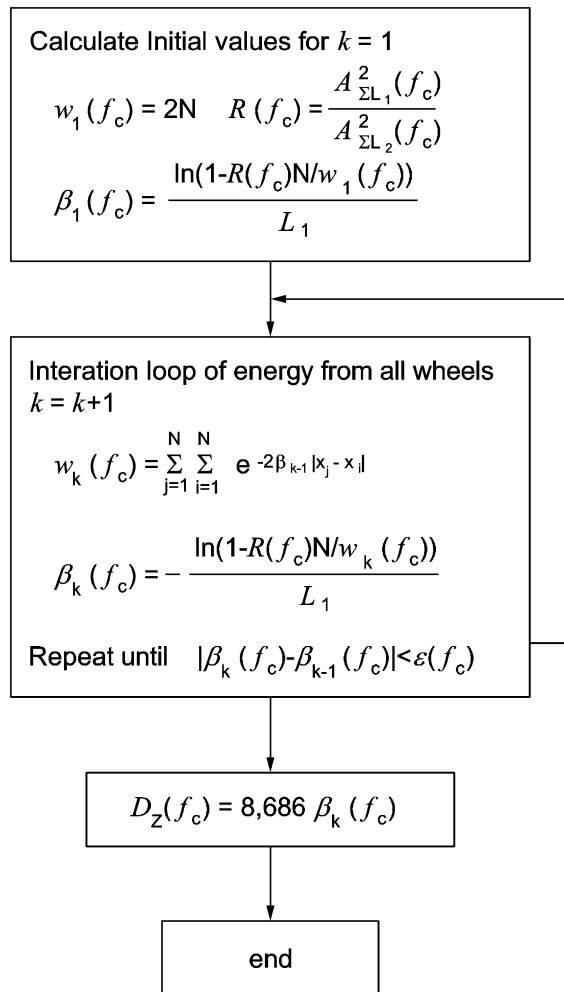
$$w_k(f_c) = \sum_{j=1}^N \sum_{i=1}^N e^{-2\beta_{k-1}|x_j - x_i|} \quad (8)$$

where

$x_j - x_i$ is the distance between the current wheel j and another wheel i

The weighting coefficient w_k represents a sum of the squared contributions from all wheels, viewed from each wheel and then summated over all wheels. If the decay exponent is large, the effect of adjacent wheels is small and w_k quickly converges to $w_k = N$. If the decay is small then w_k becomes larger. Sufficient convergence is often achieved within around four steps.

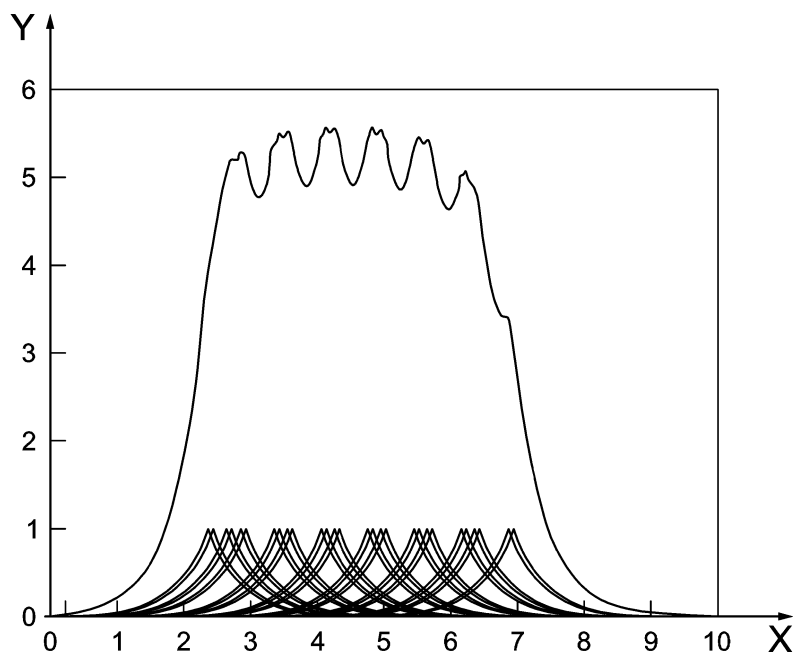
The effect of the decay rate on the exponential vibration amplitude of each wheel is shown in Figures 4a, 4b and 4c. The overlap between the amplitude envelope curves of individual wheels increases significantly for medium or low decay rates.



NOTE $\varepsilon(f_c)$ is taken at 0,1

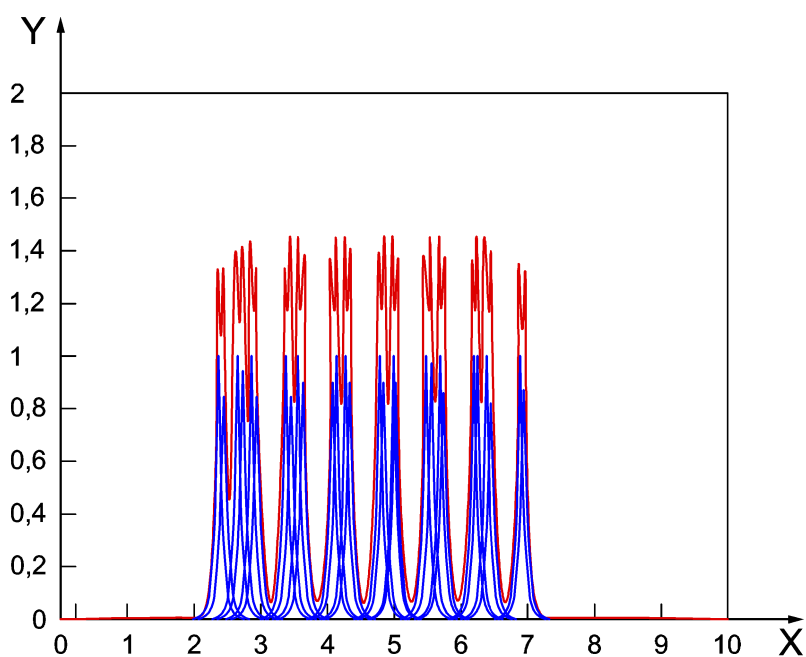
Figure 3 — Flowchart for the energy iteration procedure

Exponential pass-by envelope curves and summated curve, decay rate = 0,5 dB/m



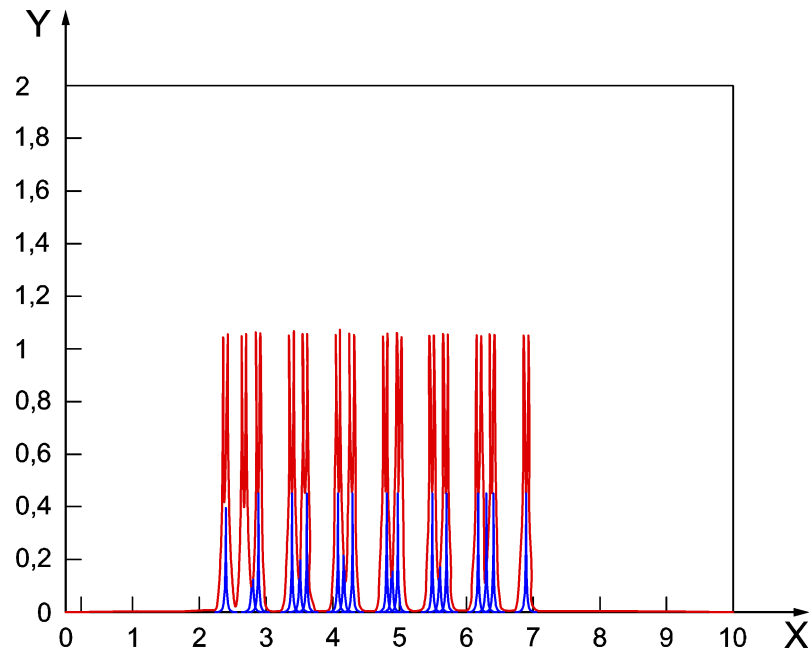
a) — Simulated envelope curves of vibration of individual wheels and summated amplitude of all wheels for low decay rates

Exponential pass-by envelope curves and summated curve, decay rate = 4 dB/m



b) Simulated envelope curves of vibration of individual wheels and summated amplitude of all wheels for medium decay rates

Exponential pass-by envelope curves and summated curve, decay rate = 10 dB/m



c) Simulated envelope curves of vibration of individual wheels and summated amplitude of all wheels for high decay rates

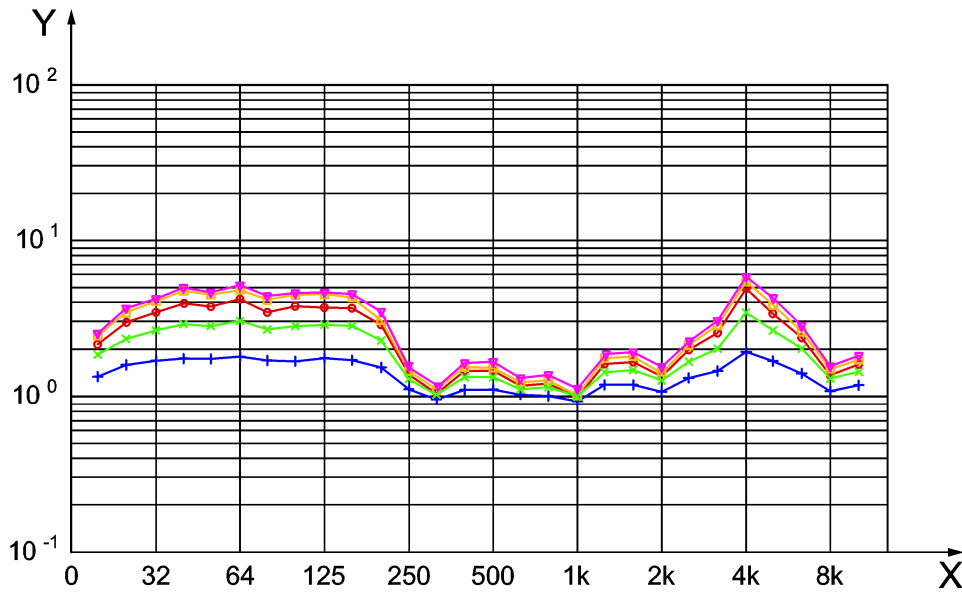
Key

Y amplitude in m/s^2

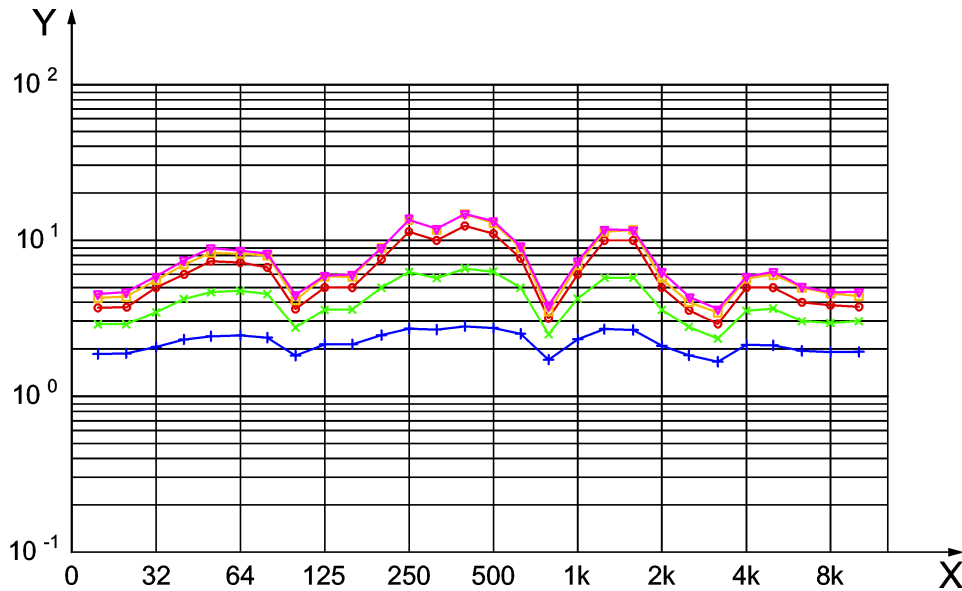
X time in s

Figure 4 — Simulated envelope curves of vibration of individual wheels and summated amplitude of all wheels

Examples of the iteration procedure are shown in Figures 5a and 5b, with convergence towards a relatively low decay rate and a high decay rate. The lowest curve is the initial value with four iteration steps above it.



a) Convergence of a decay rate applying the iteration procedure for a low decay rate



b) Convergence of a decay rate applying the iteration procedure for a higher decay rate

Key

Y track decay rate in dB/m

X frequency in Hz

NOTE The initial curve is the lowest.

Figure 5 — Convergence of a decay rate applying the iteration procedure

12 Method to determine the combined roughness from vertical railhead vibration

The combined roughness for the whole train or part of a train with length ℓ is determined by the following formula:

$$L_{\text{Rtot}}(f_c, v) = L_{\text{aeq,tp}}(f_c, v) + 10 \lg \left(\frac{D_z(f_c) \ell}{8,686 N_{\text{ax}}} \right) - A_1(f_c) - A_2(f_c) - 40 \lg(2\pi f_c) \quad (9)$$

$L_{\text{aeq,tp}}(f_c, v)$ is the equivalent acceleration spectrum in one-third octave bands measured during the pass-by of train during time t_p with length ℓ and N_{ax} axles, running at speed v .

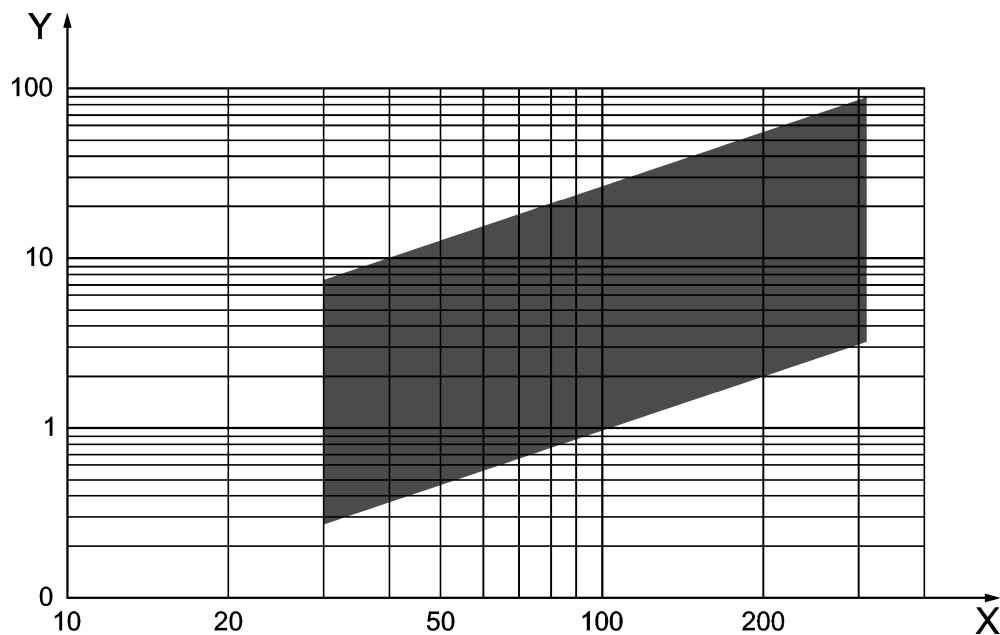
A_1 is the difference between the spectrum measured at the actual measurement position and at the railhead. It is negligible below around 4 kHz. If required, A_1 may be either calculated or measured using an impact hammer.

$A_2(f)$ is the difference between the combined roughness and the contact point displacement described in Annex A. It is tabulated in Annex A for a range of typical situations. It can also be calculated from the wheel, rail and contact point receptances if required.

The uncertainty in combined roughness can be reduced by using the average decay rate as input for the calculation of the above formula.

If the combined roughness is averaged over several pass-bys, the arithmetic mean of roughness levels shall be calculated in each one-third octave wavelength band.

The approximate range of applicability of the combined roughness method is indicated in Figure 6 in terms of train speeds and wavelengths. Smaller wavelengths are best measured at lower speeds, while larger wavelengths are better measured at higher speeds.



Key

- Y wavelength in cm
- X speed in km/h

Figure 6 — Approximate applicability range for determining combined roughness from rail vibration data during train pass-bys

13 Method to convert roughness from frequency to wavelength domain

For roughness and wavelength conventions and presentation, reference is made to EN 15610 on rail roughness measurement, with the exception of the use of the symbol L_{Rtot} for effective roughness.

When the combined effective roughness level L_{Rtot} is derived from vertical railhead vibration, it is typically a frequency spectrum $L_{Rtot}(f_c)$ determined at a given speed v . To obtain roughness as a function of wavelength λ , it shall be converted to the required speed using the relation $\lambda = v/f_c$, where f_c is the centre band frequency of a given one-third octave band in Hz and v is the train speed in m/s. The roughness spectrum as a function of frequency shifts along the frequency axis for different speeds.

Start with given frequency spectrum $L_{Rtot}(f_c)$ with standard one-third octave centre frequencies f_c . Convert each one-third octave frequency band given speed v to a corresponding wavelength band according to $\lambda = v/f_c$, so the roughness frequency spectrum is transformed into a roughness wavelength spectrum: $L_{Rtot}(\lambda)$.

The wavelengths λ that result from this transformation will generally not correspond to standard wavelengths λ_c . So to obtain the values for roughness at standard wavelengths, the roughness energy at the non-standard wavelength bands should be distributed to the standard wavelength bands. Standard octave and one-third octave wavelengths are given in Table 1.

Table 1 — Standard octave and one-third octave wavelengths

Octave band centre wavelength [mm] $\lambda_{c,oct}$	Third octave band centre wavelength [mm]		
	$\lambda_{c,third,1}$	$\lambda_{c,third,2}$	$\lambda_{c,third,3}$
500	630	500	400
250	315	250	200
125	160	125	100
63	80	63	50
31,50	40	31,50	25
16	20	16	12,50
8	10	8	6,30
4	5	4	3,15
2	2,50	2	1,60
1	1,25	1	0,80

To obtain roughness values at the preferred standard wavelengths λ_c the roughness levels derived at the neighbouring wavelengths around a certain desired standard wavelength are used. First the neighbouring wavelengths resulting from the frequency-to-wavelength transformation are located, which are named λ_- and λ_+ such that $\lambda_- < \lambda_c < \lambda_+$. Now the roughness level at wavelength λ_c can be calculated with:

$$L_{Rtot}(\lambda_c) = 10 \log \left\{ \frac{\lambda_- - \lambda_{-cl}}{\lambda_- - \lambda_{-l}} 10^{\frac{L_{Rtot}(\lambda_-)}{10}} + \frac{\lambda_{cu} - \lambda_{+l}}{\lambda_{+u} - \lambda_{+l}} 10^{\frac{L_{Rtot}(\lambda_+)}{10}} \right\} \quad (10)$$

where

l denotes the lower limit of the corresponding wavelength band;

u denotes the upper limit of the corresponding wavelength band.

The band limits for one-third octave bands can be obtained from the centre wavelengths as follows:

$$\lambda_{cl} = \frac{1}{\sqrt[3]{2}} \lambda_c \text{ and } \lambda_{cu} = \sqrt[3]{2} \lambda_c \quad (11)$$

This is valid for the preferred standard wavelengths as well as for the neighbouring wavelengths. By substituting (11) in (10) the following expression for $L_{Rtot}(\lambda_i)$ is obtained:

$$L_{Rtot}(\lambda_c) = 10 \lg \left\{ \frac{\lambda_+ - \lambda_c}{\lambda_+ - \lambda_-} 10^{\frac{L_{Rtot}(\lambda_-)}{10}} + \frac{\lambda_c - \lambda_-}{\lambda_+ - \lambda_-} 10^{\frac{L_{Rtot}(\lambda_+)}{10}} \right\} \quad (12)$$

In this way, the roughness 'energy' of the neighbouring wavelength bands is proportionally attributed to the standard wavelength band as shown in Figure 7.

It should be noted that a correct conversion is only possible using the exact centre wavelengths λ_c and centre frequencies f_c , as defined in EN ISO 266. Using the nominal centre wavelengths in Table 1 for the conversion leads to an overlapping of wavelength bands and a small error regarding the conservation of energy in the order of 1 % or less.

It may be required to have measurements at more than one speed so as to obtain a sufficient wavelength range for a particular application. Roughness spectra from multiple measurements may be averaged over common wavelengths, omitting or including points outside the common wavelength range.

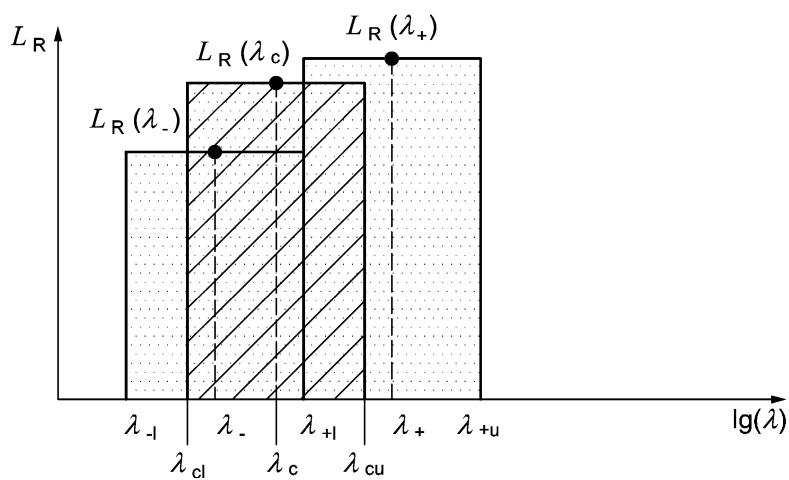
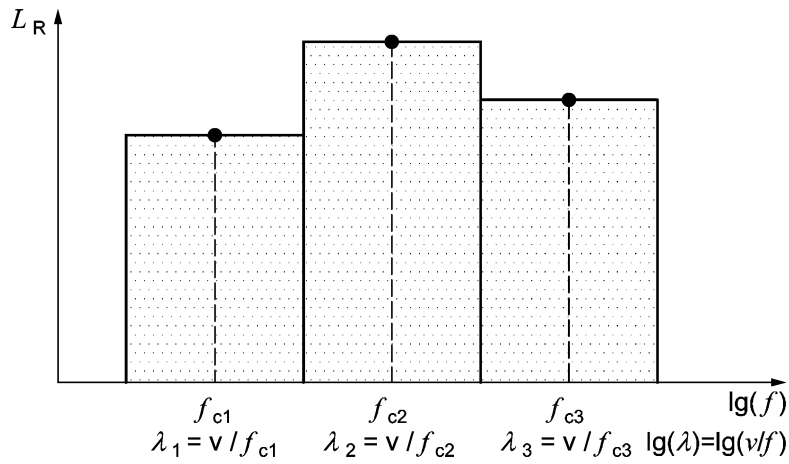


Figure 7 — Illustration of roughness spectrum conversion from frequency to wavelength spectrum

14 Method to determine the rolling noise transfer function

14.1 Definition

If rolling noise is the only significant source during a train pass-by (from absence of aerodynamic, traction or impact noise sources), then the total rolling noise transfer function is determined from the equivalent sound pressure level and combined roughness at speed v , and normalized to the axle density N_{ax}/ℓ (equivalent to APL in the Noise TSI [1]):

$$L_{HpR_{tot,nl}}(f_c) = L_{peq,tp}(f_c) - L_{R_{tot}}(f_c, v) - 10 \lg(N_{ax} / \ell) \quad (13)$$

The total transfer function $L_{HpR_{tot,nl}}(f_c)$ is independent from the roughness, train length and number of axles. It characterizes the vibroacoustic properties of the vehicle, the track and the propagation path.

A transfer function can also be defined in terms of sound power which is given for a defined length of track or vehicle and is normalized to the number of axles:

$$L_{\text{HWRtot},n}(f_c) = L_{\text{W}}(f_c) - L_{\text{Rtot}}(f_c, v) - 10 \lg(N_{\text{ax}}) \quad (14)$$

where

$L_{\text{W}}(f_c)$ is the sound power level of the vehicle (therefore dependent on the length).

If the transfer function is determined from several pass-bys, averaging is done arithmetically.

14.2 Application examples

The total transfer function can also be split into a vehicle component and a track component, using separation methods based on calculation, reference vehicles or tracks or stationary reciprocal measurements. See [2] and [3].

It can also be used to separate rolling noise from other sources, for example aerodynamic noise from rolling noise or traction noise from rolling noise. See [5] and [6].

The definition of transfer function in terms of sound power given above corresponds to the EU-calculation method described in [12].

15 Test report

The results of decay rate analysis shall be presented as specified in EN 15461. The results of combined roughness analysis shall be reported as specified in EN 15610 except for the quantity symbol which is L_{Rtot} instead of L_{r} . Transfer functions shall be presented in the same manner as sound pressure level spectra in one-third octave bands, as specified in EN ISO 266. The reference value for the transfer function is 20 [Pa/m^{0,5}] for $L_{\text{HpRtot},n1}$ and 1 [W/m²] for $L_{\text{HWRtot},n}$.

16 Uncertainty and grade

The uncertainty in decay rates, combined roughness and transfer functions determined according to the iteration method is estimated at ± 3 dB in one-third octave bands, assuming averaging over at least three pass-bys. The main influence factors are specified in Table 2.

The combined roughness is only valid for the actual contact position of wheel and rail, and therefore may sometimes differ from direct roughness measurements. The combined roughness is representative for the selected measurement point along the rail. If strong rail roughness variation is expected along the rail, the corresponding uncertainty can be reduced by including more measurement points along the rail.

The grade is considered engineering grade if averaging over several pass-bys is applied, as described in the method. Analysis results from single pass-bys may be of survey grade or better.

Table 2 — Influence factors affecting uncertainty

Factors	Remarks	Formula or range
decay rate		
vertical rail vibration	include sufficient time signal, e.g. at least - 10 dB points ahead of and behind train	
train speed	if too low, signal level may be insufficient	
integration time around wheels and over whole signal, or vibration ratio $R(f_1)$	may depend on selection points or signal quality	
combined roughness		
vertical rail vibration	directly proportional	ΔL_{Rtot} approximately ΔL_a
decay rate	directly proportional	ΔL_{Rtot} approximately ΔD_z
train speed	averaging over two or more speeds is recommended; speed error shifts L_R curve	$\Delta L_{Rtot}(f_c)$ approximately $\Delta v \frac{dL_{Rtot}}{dm_c}$ $m_c =$ band number
A_2 factor	see Annex A	max. ± 3 dB
transfer function		
combined roughness	directly proportional	ΔL_H approximately $-\Delta L_{Rtot}$
sound pressure level	directly proportional	ΔL_H approximately ΔL_p

Annex A (informative)

A₂ factor, difference between the combined roughness and the contact point displacement

The A₂ factor can be determined from the ratio of rail receptance α_{rail} and the sum of wheel, rail and contact receptances α_{wheel} , α_{rail} and α_{contact} :

$$A_2 = 20 \lg \left(\frac{|\alpha_{\text{rail}}|}{(|\alpha_{\text{rail}}| + \alpha_{\text{wheel}} + \alpha_{\text{contact}})} \right) \quad (\text{A.1})$$

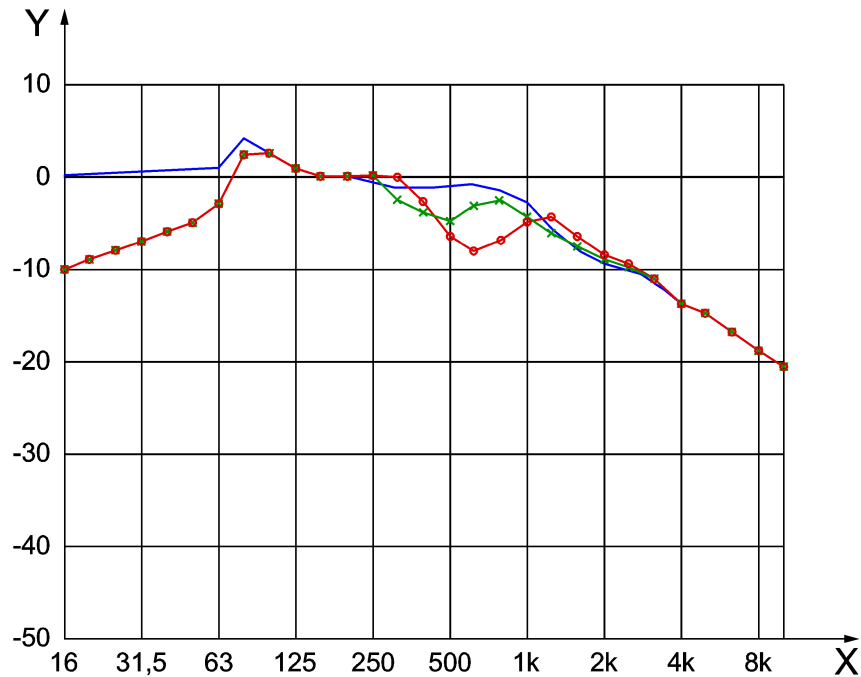
Example spectra for the A₂ factor have been determined for a range of typical parameter values using the TWINS software [9]. The reference situation consisted of a standard UIC 920 mm diameter freight wheel, a track with UIC 60 rails, bibloc sleepers at 0,6 m spacing and rail pads of (loaded) stiffness 400 MN/m. The (loaded) ballast stiffness is set to 100 MN/m per sleeper end. The influences of pad stiffness, ballast stiffness, sleeper type, contact position on rail and wheel, wheel load and wheel type on the spectrum A₂ were evaluated. The pad stiffness is shown to be the most influential parameter. In the frequency range from 100 Hz to 3 150 Hz inclusive, the spectrum A₂ can be determined to an accuracy of ± 3 dB for application to conventional wheels, provided that the rail pad stiffness can be allocated to one of the three categories, as listed in Table A.1 and graphed in Figure A.1. This makes the uncertainty of the combined roughness estimation no smaller than that of the direct method with a stylus. To increase the accuracy of the prediction of the combined effective roughness, several measurements with different train speeds should be averaged. This results in the peaks and dips in frequency spectrum A₂ spreading out over a wider wavelength range.

The tabulated values for A₂ given here are not applicable to situations where rail and wheel geometry and design differ significantly from conventional rail, for example small wheels and light rail with resilient wheels. In these situations the A₂ factor should be determined either by measurement and/or calculation.

For ballastless track systems with soft support the A₂ factor given for soft pads can be used.

Table A.1 — One-third octave spectra $A_2(f_c)$ in dB for three categories of rail pad stiffness

Frequency [Hz]	Soft	Medium	Stiff
63	1,0	- 3,0	- 3,0
80	4,1	2,3	2,3
100	2,7	2,6	2,6
125	0,9	0,8	0,8
160	0,1	0,0	0,0
200	0,0	0,0	0,0
250	- 0,6	0,0	0,2
315	- 1,2	- 2,6	- 0,1
400	- 1,3	- 3,9	- 2,8
500	- 0,9	- 4,8	- 6,5
630	- 0,9	- 3,2	- 8,1
800	- 1,6	- 2,6	- 6,9
1 000	- 2,7	- 4,3	- 5,0
1 250	- 5,6	- 6,2	- 4,4
1 600	- 8,0	- 7,5	- 6,4
2 000	- 9,5	- 8,8	- 8,4
2 500	- 10,0	- 9,8	- 9,5
3 150	- 11,3	- 11,2	- 11,1
4 000	- 13,7	- 13,6	- 13,6
5 000	- 14,9	- 14,8	- 14,8



Key

Y	A_2 in dB	Medium
X	frequency in Hz	Stiff
	Soft	

Figure A.1 — A_2 factor for different characteristic railpad stiffnesses

Table A.2 — Ranges of pad stiffness applying to different categories of pads used in defining standard spectra for A_2

Sleeper	Soft support	Medium support	Stiff support
Bibloc sleepers	≤ 400 MN/m	400 – 800 MN/m	≥ 800 MN/m
Monobloc sleepers	≤ 800 MN/m	≥ 800 MN/m	–
Wooden sleepers	all	–	–

The selection of soft, medium or stiff pad depends on the sleeper type.

For wooden sleepers the values for ‘soft’ pads are applied. Different pad stiffness ranges apply to bibloc and monobloc sleepers as shown in Table A.2. As in practice the actual pad stiffness is not always known, an assumed equivalent stiffness can be based on the shape of the vertical decay rate curve. The frequency at which it tends to drop down, see for example the 1 kHz band in Figure B.1, can be used as an indication for the pad stiffness as shown in Table A.3.

Depending on the data quality it may be possible to automate this process.

Table A.3 — Frequencies [Hz] at which the decay rate of vertical rail vibration falls below 4 dB/m for various values of pad stiffness (from [9])

Sleeper	80 MN/m	200 MN/m	400 MN/m	800 MN/m	1 250 MN/m	2 000 MN/m
Bibloc sleepers	300	480	710	1 060	1 400	1 950
Monobloc sleepers	280	250	610 – 850	1 100 – 1 380	1 630	2 040

Annex B (informative)

Benchmark examples and background information

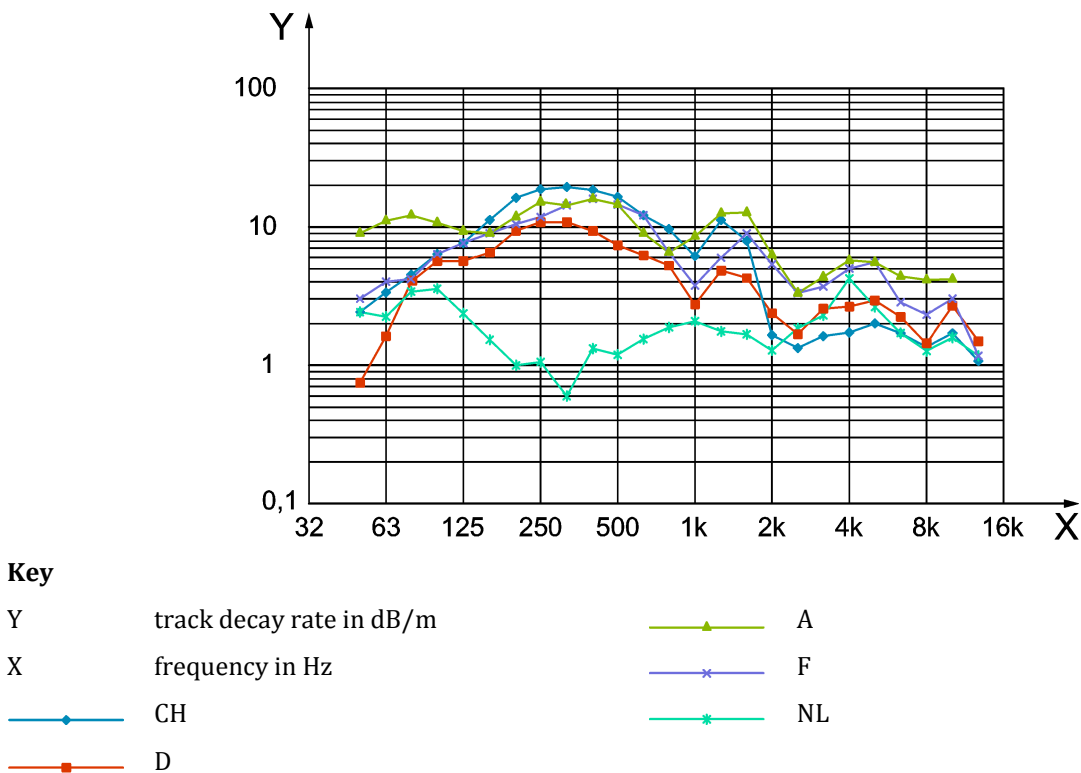
B.1 General

This annex provides examples of analysis results of benchmark data from several countries, illustrating performance of different analysis methods, and for the energy iteration method the repeatability, reproducibility, effect of accelerometer position, train speed, averaging and other aspects.

As the vertical track decay rate is a key input parameter to determine combined roughness, a large part of the examples are focused on this.

Many of the results of track decay rate analysis are taken from a benchmark study [7], [8] on a number of data sets from France, Germany, The Netherlands, Austria and Switzerland.

B.2 Examples of vertical decay rates determined for several different tracks



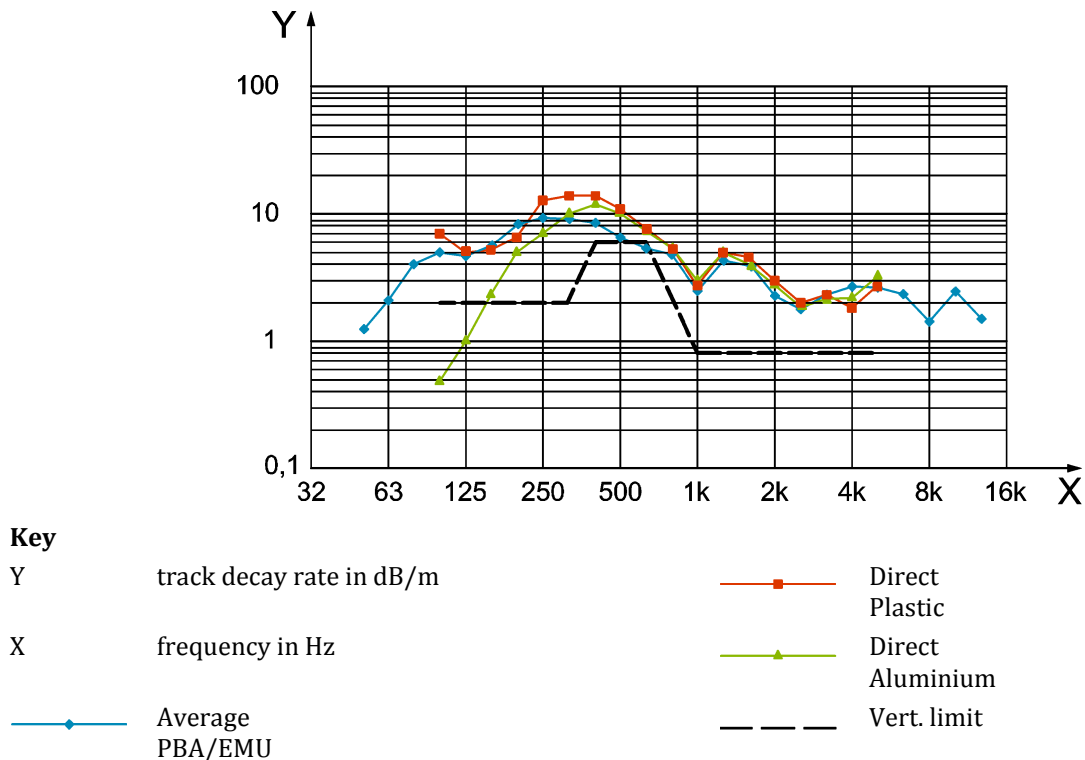
NOTE In Figure B.1 the vertical track decay rates included in the benchmark data from five different sites are set out. The Swiss, German and Austrian tracks were ballasted with monobloc sleepers, the French track had bibloc sleepers and the Dutch track was a ballastless track system with very soft pads.

Figure B.1 — Vertical track decay rates included in the benchmark data from five different sites

B.3 Comparison with direct measurements

Although track decay rates determined from hammer measurements on unloaded track and from rail vibration measurements during a train pass-by can be expected to differ somewhat due to loading, nevertheless, generally a good comparison is found. Some examples are given in the Figures B.2, B.3, B.4, B.5, B.6, B.23 and Figure B.24. In cases where differences are found this can be due to loading of the track, temperature effects or analysis errors.

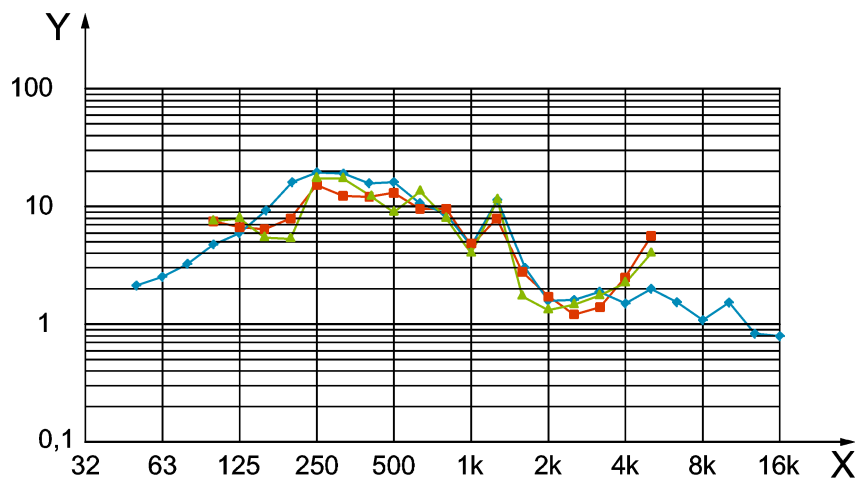
For combined roughness, the differences with summated direct roughness can be larger due to the potential difference in line of contact along the rail.



NOTE 1 The pass-by result was averaged over a total of 24 pass-bys of an EMU 2 and an EMU 4 car train travelling at 60 km/h, 80 km/h and 160 km/h.

NOTE 2 The hammer measurements were performed with plastic and aluminium heads.

Figure B.2 — Comparison of track decay rate from the pass-by energy iteration method and direct measurements on a German ballasted track with monobloc sleepers

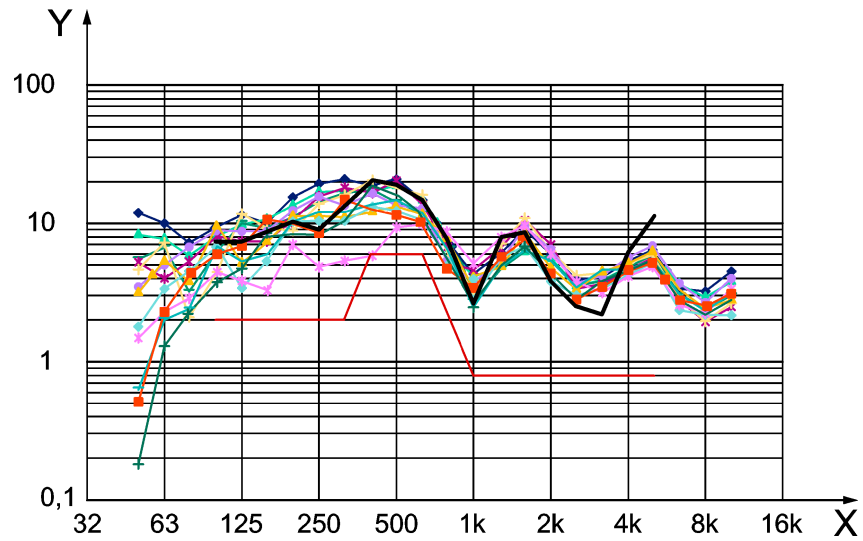


Key

Y	track decay rate in dB/m	—■—	Direct A
X	frequency in Hz	—▲—	Direct B
—◆—	PBA Average		

NOTE The pass-by result was averaged over seven pass-bys.

Figure B.3 — Comparison of vertical track decay rates from the pass-by energy iteration method and from direct measurement on a Swiss ballasted track with monobloc sleepers

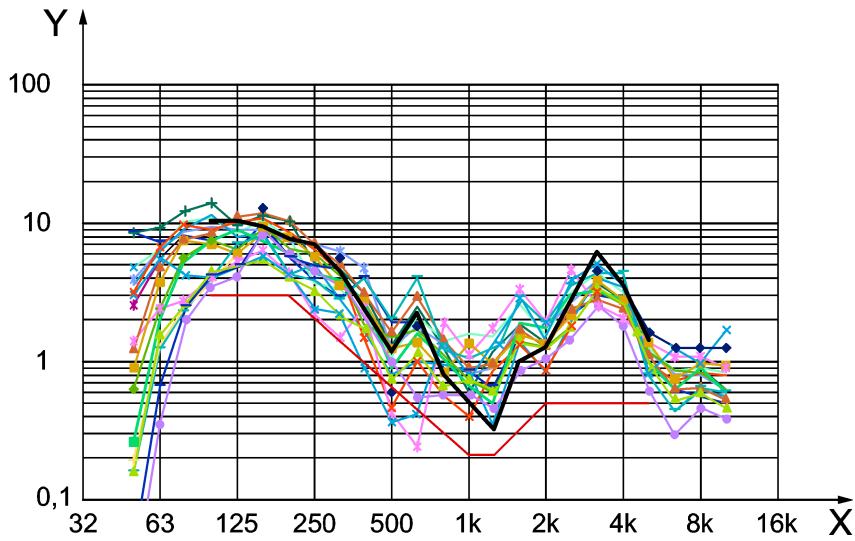


Key

Y	track decay rate in dB/m		Pby008 V2_1
X	frequency in Hz		Pby009 V1_1
	TSI Vert Limit		Pby009 V2_1
	Pby001 V2		Pby010 V1_1
	Pby002 V2_3		Pby010 V2_1
	Pby003 V2_1		Pby011 V1_1
	Pby004 V2_1		Pby011 V2_1
	Pby005 V2_1		Pby012 V1_1
	Pby006 V2_2		Pby012 V2_1
	Pby007 V2_2		AEIF Impact
	Pby008 V1_1		

NOTE A series of pass-bys was processed with different trains and at various speeds.

Figure B.4 — Comparison of vertical track decay rates from the pass-by energy iteration method (Pbyxxx) and from direct measurement on a French ballasted track with bibloc sleepers

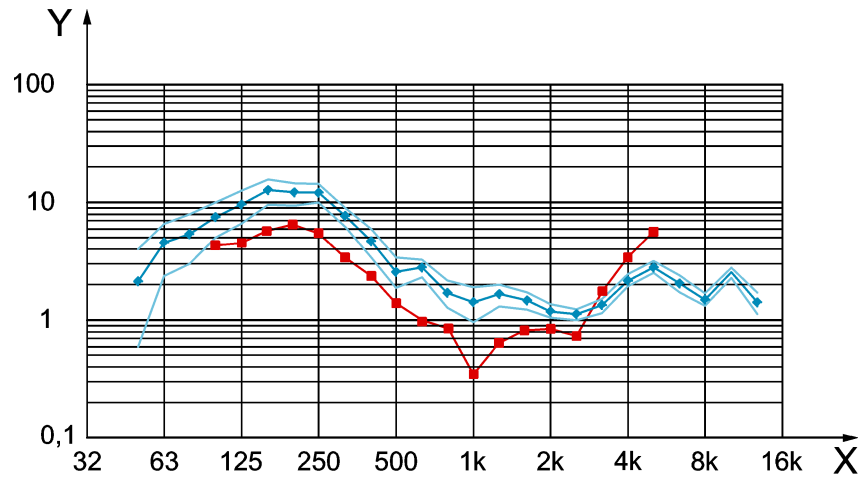


Key

- | | | | |
|---|--------------------------|--|-------------|
| Y | track decay rate in dB/m | | |
| X | frequency in Hz | | |
| | TSI Lat Limit | | Pby006 L2_1 |
| | Pby001 L1 | | Pby007 L1_1 |
| | Pby001 L2 | | Pby007 L2_1 |
| | Pby002 L2_3 | | Pby008 L1_1 |
| | Pby002 L1_3 | | Pby008 L2_1 |
| | Pby003 L1_1 | | Pby009 L1_1 |
| | Pby004 L1_1 | | Pby009 L2_1 |
| | Pby004 L2_1 | | Pby010 L1_1 |
| | Pby005 L1_1 | | Pby011 L1_1 |
| | Pby005 L2_1 | | Pby011 L2_1 |
| | Pby006 L1_1 | | Pby012 L1_1 |
| | | | Pby012 L2_1 |
| | | | AEIF Impact |

NOTE A series of pass-bys was carried out with different trains and at various speeds.

Figure B.5 — Comparison of lateral track decay rates from the pass-by energy iteration method (Pbyxxx) and from direct measurement on a French ballasted track with bibloc sleepers



Key

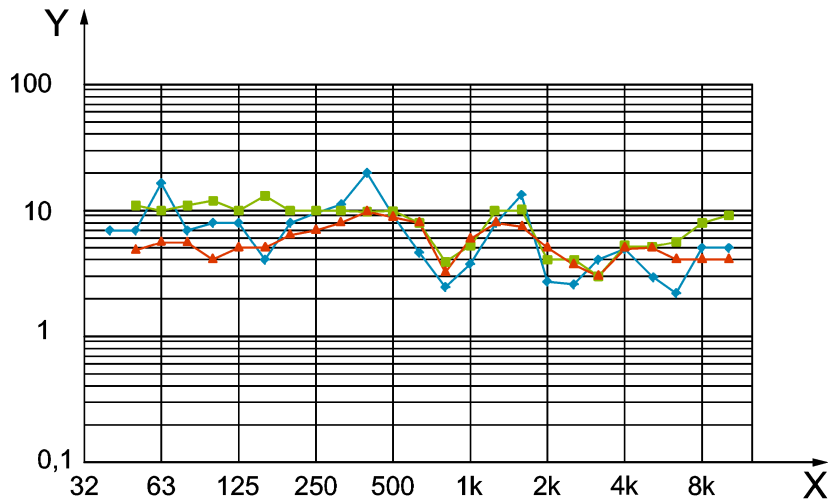
Y	track decay rate in dB/m	—————	Indirect+
X	frequency in Hz	—————	Indirect-
—◆—	Indirect	—■—	Direct

NOTE A series of pass-bys was processed with a test train at various speeds and the results were then averaged. The standard deviation corresponds to curves indicated with + and -. Temperature and/or loading effects may explain the difference seen here.

Figure B.6 — Comparison of vertical track decay rates from the pass-by energy iteration method and from direct measurement on a German ballasted track with bibloc sleepers

B.4 Comparison of TDR methods

Results for the manual slope method, the automatic derivative slope method and the energy iteration method are shown in Figure B.7 for a track with high decay rate and for a track with low decay rate in Figure B.8.

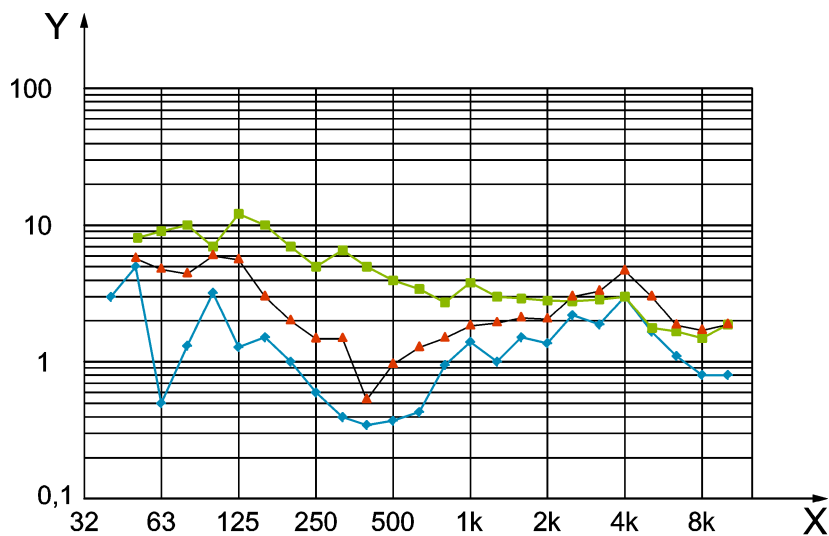


Key

Y	track decay rate in dB/m		Slope derivative max.
X	frequency in Hz		Energy
	Manual slope		

NOTE Results corresponding to a single pass-by at a speed of 121 km/h.

Figure B.7 — Vertical track decay rates determined by manual slope method, slope derivative method and energy iteration method on a monobloc sleeper track with high decay rate



Key

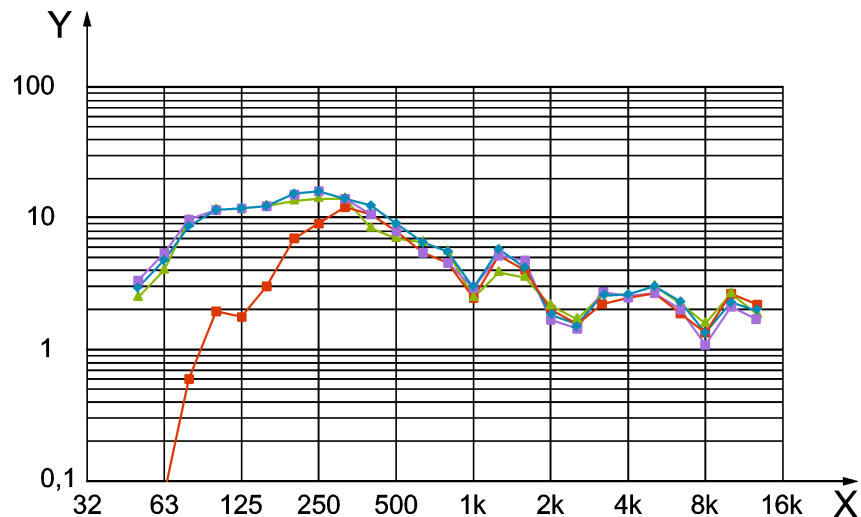
Y	track decay rate in dB/m		Slope derivative max.
X	frequency in Hz		Energy
	Manual slope		

NOTE Results corresponding to a single pass-by at a speed of 148 km/h.





Figure B.8 — Vertical track decay rates determined by manual slope method, slope derivative method and energy iteration method on slab track with soft baseplates used on the NL HSL

B.5 Repeatability

Repeatability of the track decay rate using the energy iteration method is illustrated for a monobloc sleeper track and for a ballastless track system with soft pads. In Figure B.9 and Figure B.10 the analysis was repeated on the same pass-by data. In Figure B.11 and Figure B.12 analysis were performed on several pass-bys of the same train at one speed. The outlier curves are due to too short a total integration time and should be rejected.



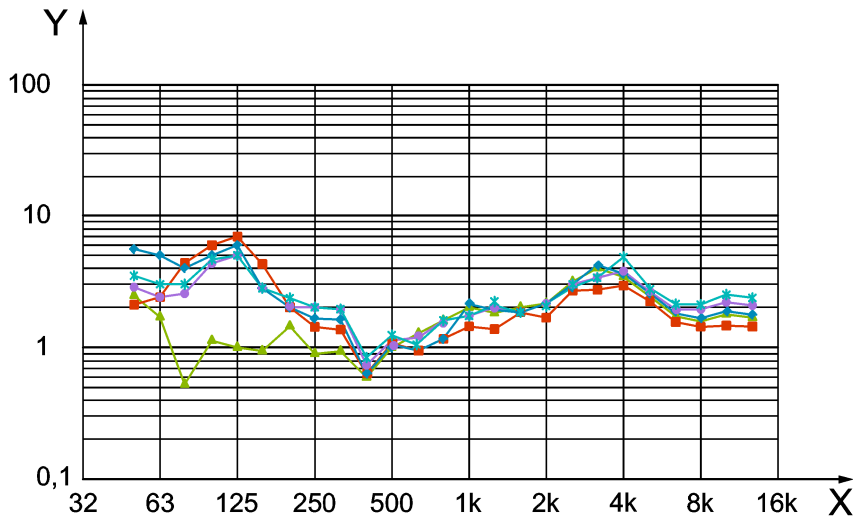
Key

Y	track decay rate in dB/m		#2
X	frequency in Hz		#3
	#1		#4

NOTE 1 Results corresponding to a pass-by of an EMU 2 car at 80 km/h.

NOTE 2 The analysis was repeated four times on the same pass-by data.

Figure B.9 — Vertical track decay rate determined on a German ballasted track with monobloc sleepers



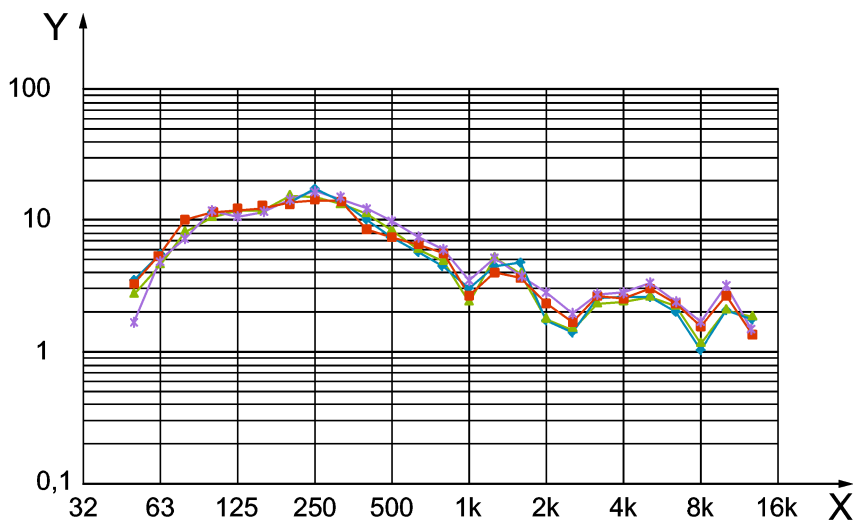
Key

Y	track decay rate in dB/m		#3
X	frequency in Hz		#4
	#1		#5
	#2		

NOTE 1 Results corresponding to the pass-by of an Intercity travelling at 148 km/h.

NOTE 2 The analysis was repeated five times on the same pass-by data.

Figure B.10 — Vertical track decay rate determined on a slab track with soft baseplates used on the NL HSL

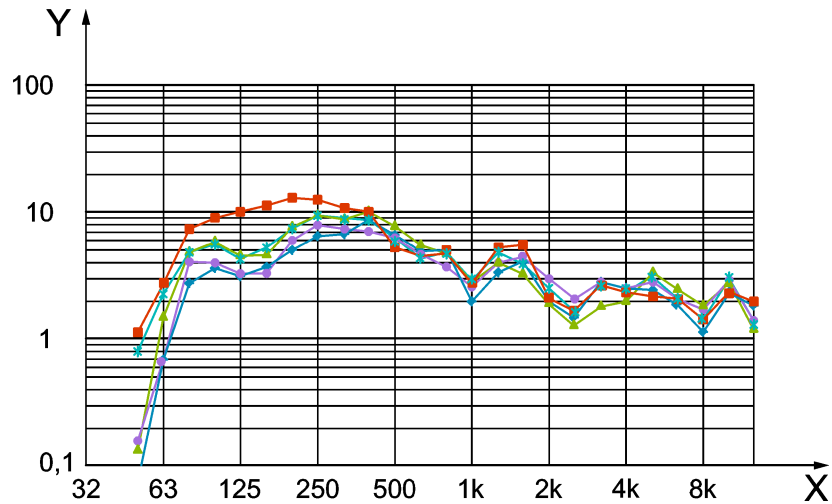


Key

Y	track decay rate in dB/m		#2
X	frequency in Hz		#3
	#1		#4

NOTE Results corresponding to four pass-bys of an EMU 2 car train travelling at 80 km/h.

Figure B.11 — Vertical track decay rate determined on a German track with monobloc sleepers



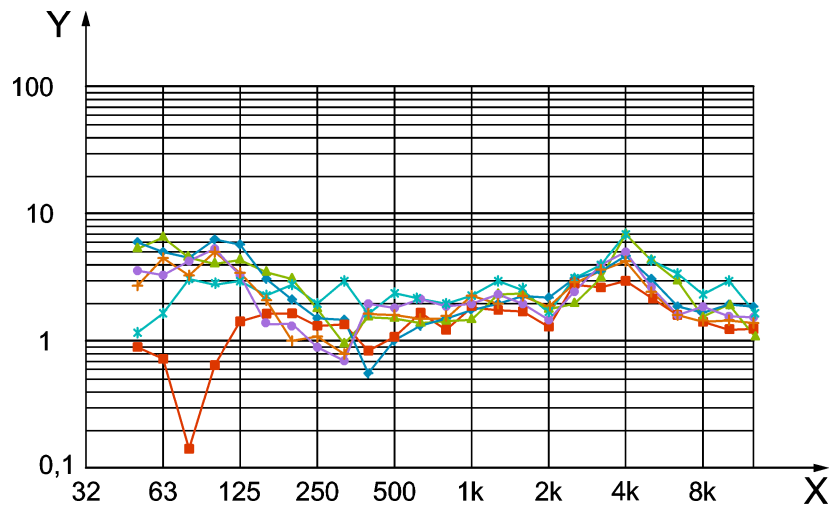
Key

Y	track decay rate in dB/m		2-1a
X	frequency in Hz		2-5a
	1-4a		2-6a
	1-7a		

NOTE Results corresponding to five pass-bys of an EMU 2 car train travelling at 160 km/h.

Figure B.12 — Vertical track decay rate determined on a German track with monobloc sleepers

The repeatability of the track decay rate from the energy iteration method for different pass-bys at the same site and a single operator is illustrated in Figure B.13 below. The outlier curves should be rejected.



Key

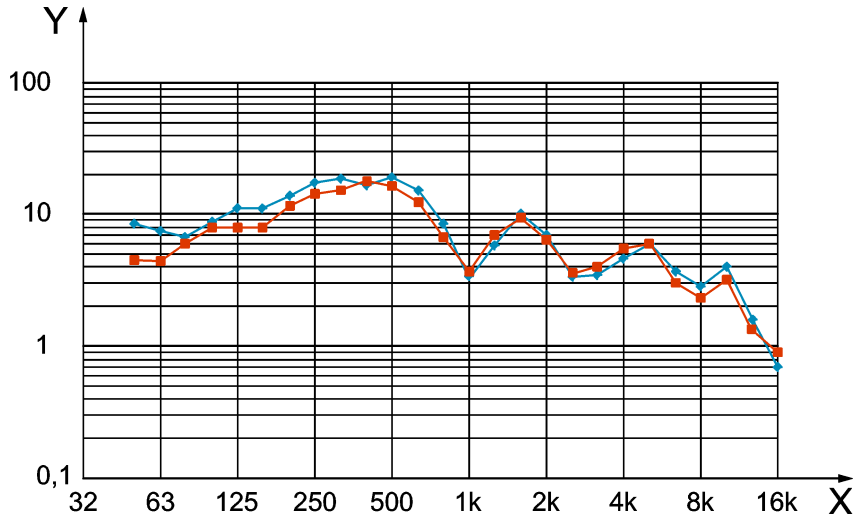
Y	track decay rate in dB/m		pb3
X	frequency in Hz		pb4
	pb1		pb5
	pb2		pb6

NOTE Results corresponding to six different pass-bys at speeds between 148 km/h and 160 km/h

Figure B.13 — Vertical track decay rates determined by the energy iteration method on slab track with soft baseplates used on the NL HSL

B.6 Reproducibility

The reproducibility of track decay rates determined with the energy method is illustrated for different train types at the same track location. In Figure B.14, Figure B.15 and Figure B.16 results are shown for different train types averaged over multiple pass-bys, on different track systems on French, Dutch and Austrian networks.



Key

Y track decay rate in dB/m

X frequency in Hz

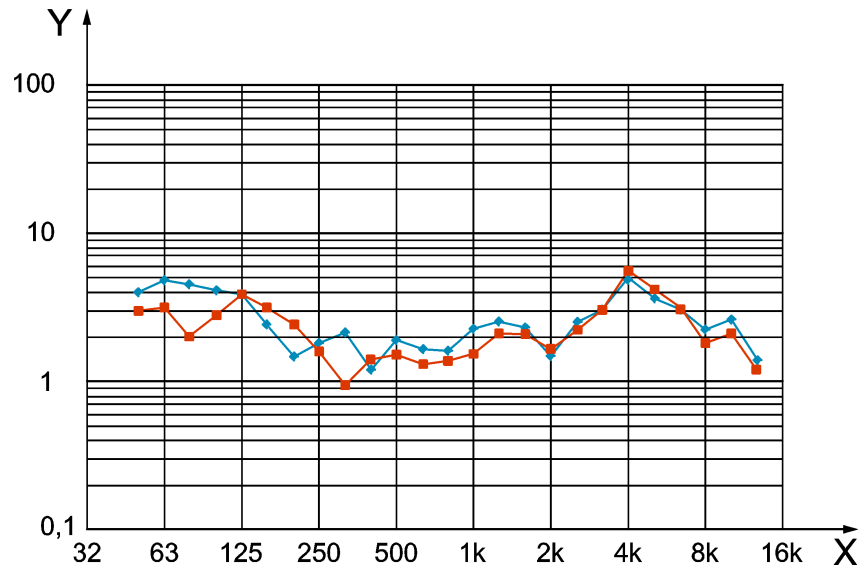
—◆— Freight

—■— EMU type ZTER

NOTE 1 Results corresponding to pass-bys of two different train types at speeds between 100 km/h and 120 km/h.

NOTE 2 The results were averaged over multiple pass-bys.

Figure B.14 — Vertical track decay rate determined with the energy method on a French bibloc sleeper ballasted track



Key

Y track decay rate in dB/m

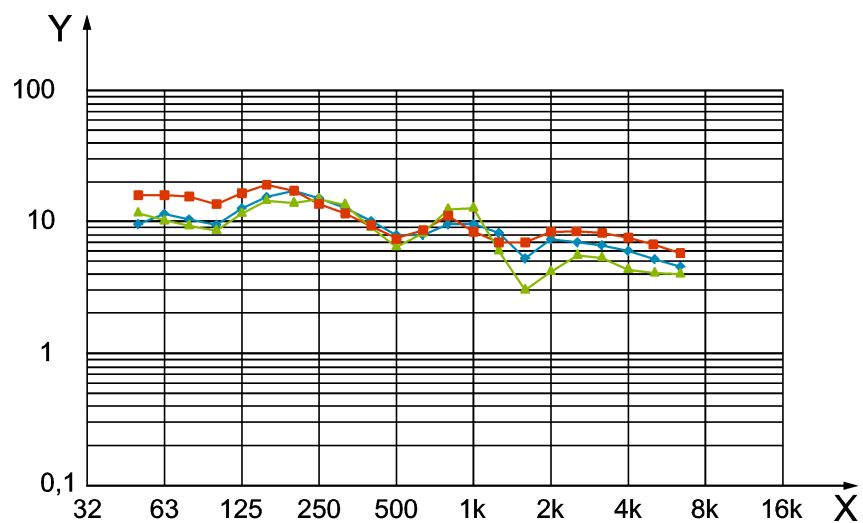
—◆— Average IC

X frequency in Hz

—■— Average Highspeed train

NOTE Results corresponding to pass-bys of Intercity and high-speed trains at 160 km/h and then averaged.

Figure B.15 — Vertical track decay rate determined with the energy method on a Dutch Rheda ballastless track system



Key

Y track decay rate in dB/m

—■— Passenger mixed

X frequency in Hz

—▲— Passenger Similar

—◆— EMU-DMU

NOTE Results corresponding to pass-bys of three different train types at 120 km/h

Figure B.16 — Vertical track decay rate determined with the energy method on an Austrian track with ballast and monobloc sleepers

The reproducibility for two different analysts is shown in Figure B.17 and Figure B.18. It is seen that differences occur mainly at low frequency, indicating the importance of the selection of the integration

range of the time signal. Results for combined roughness and transfer functions are given in Figure B.19 and Figure B.20, respectively.

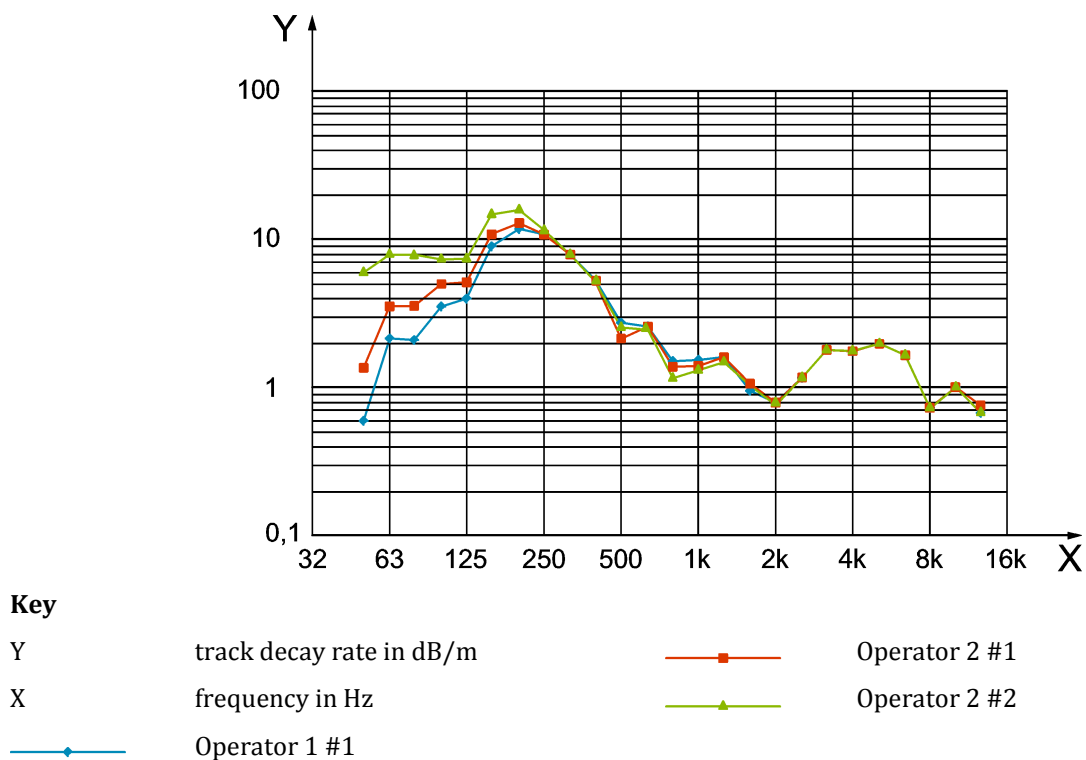
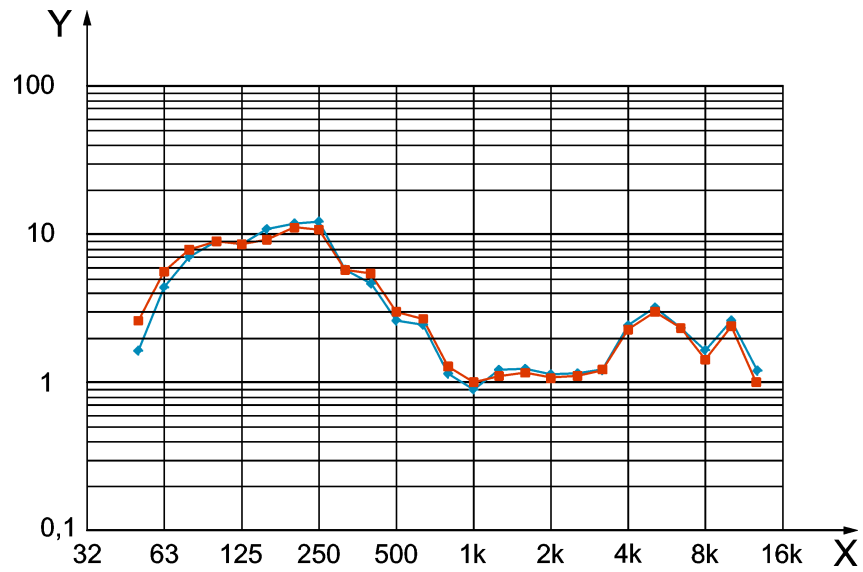


Figure B.17 — Vertical track decay rate determined by three different analysts at one company using the same method and software to process data from a German track

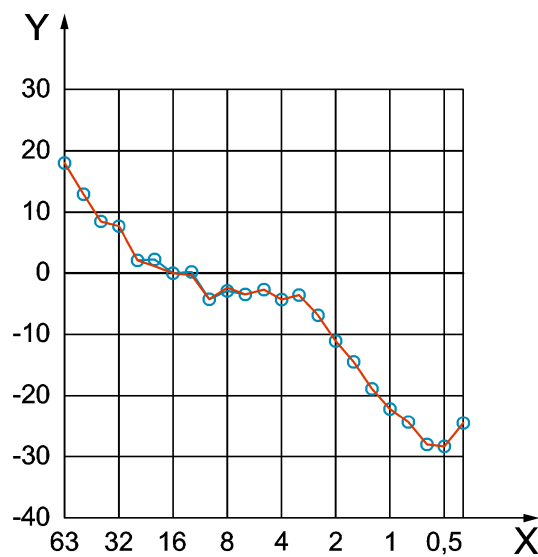


Key

- Y track decay rate in dB/m —◆— Analyst 1
- X frequency in Hz —■— Analyst 2

NOTE A single pass-by was carried out at 120 km/h.

Figure B.18 — Vertical track decay rate determined by two different analysts at different companies using the same method and software with data from a German track

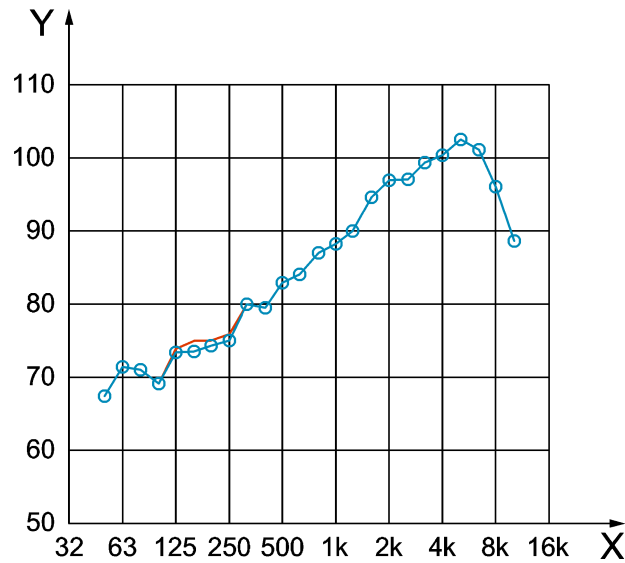


Key

- Y L_R in dB re 1µm —○— Analyst 1
- X wavelength in cm —○— Analyst 2

NOTE Results corresponding to a single pass-by of a test train at 120 km/h.

Figure B.19 — Combined roughness determined by two different analysts at different companies using the same method and software to process data from a German track (T3, 4-3b)



Key

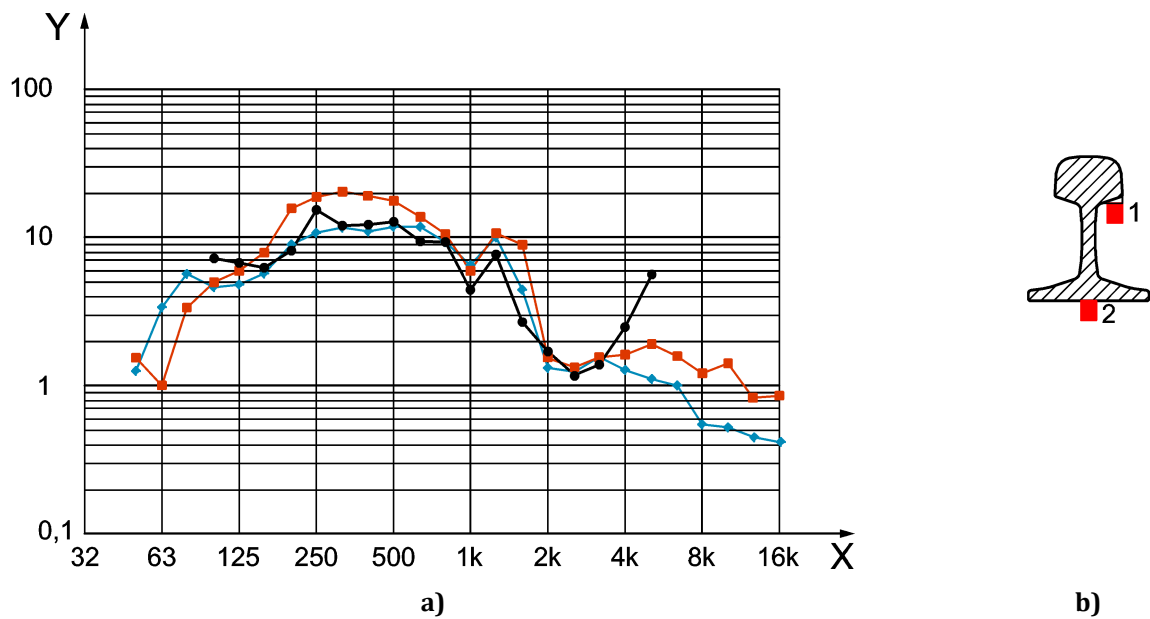
Y $L_{Hpr,nl}$ in dB re 20 Pa/ \sqrt{m} —○— Analyst 1
 X frequency in Hz — Analyst 2

NOTE Results corresponding to a single pass-by was of a test train at 12 km/h.

Figure B.20 — Total transfer function determined by two different analysts at different companies using the same method and software to process data from a German track (T3, 4-3b)

B.7 Effect of accelerometer position

The position of the accelerometer can affect the results of the decay rate, especially at higher frequencies where more wavetypes occur in the rail with cross-section deformation. In Figure B.21 below the difference between a point directly underneath the side of the railhead is compared with a point underneath the centre of the rail foot. A similar result is shown in Figure B.24.



Key

Y track decay rate in dB/m

X frequency in Hz

1 accelerometer positioned under the side of the rail head

2 accelerometer positioned under the centre of the rail foot

—◆— Acc #1

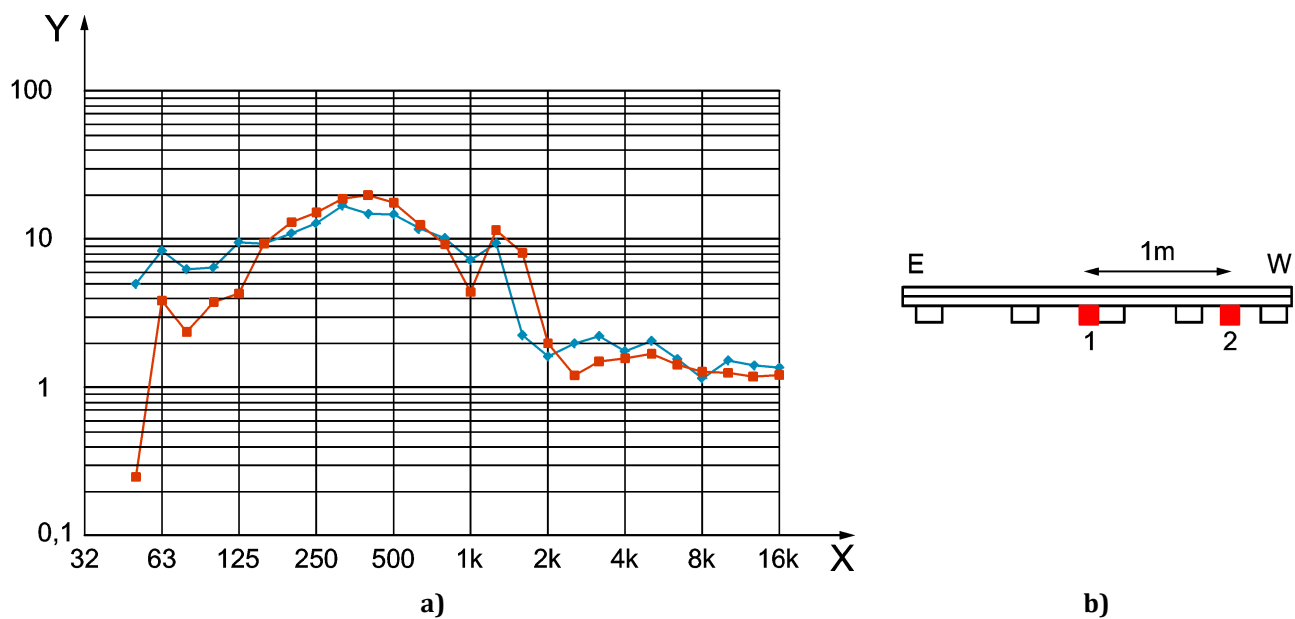
—■— Acc #2

—●— Direct

Figure B.21 — Average vertical track decay rate for two accelerometers together with the track decay rate determined from a direct measurement on a Swiss track, ballasted and with monobloc sleepers

Also the position along the rail close to or in between sleepers can affect the result. Comparisons made at two different speeds and train types are shown in Figure B.22, Figure B.23, Figure B.24 and Figure B.25 below. The difference due to position along the rail is smallest for soft railpads, which have weaker pinned-pinned resonances than rails on stiff mounting.

An example of the effect on combined roughness is set out in Figure B.26.



Key

Y track decay rate in dB/m

X frequency in Hz

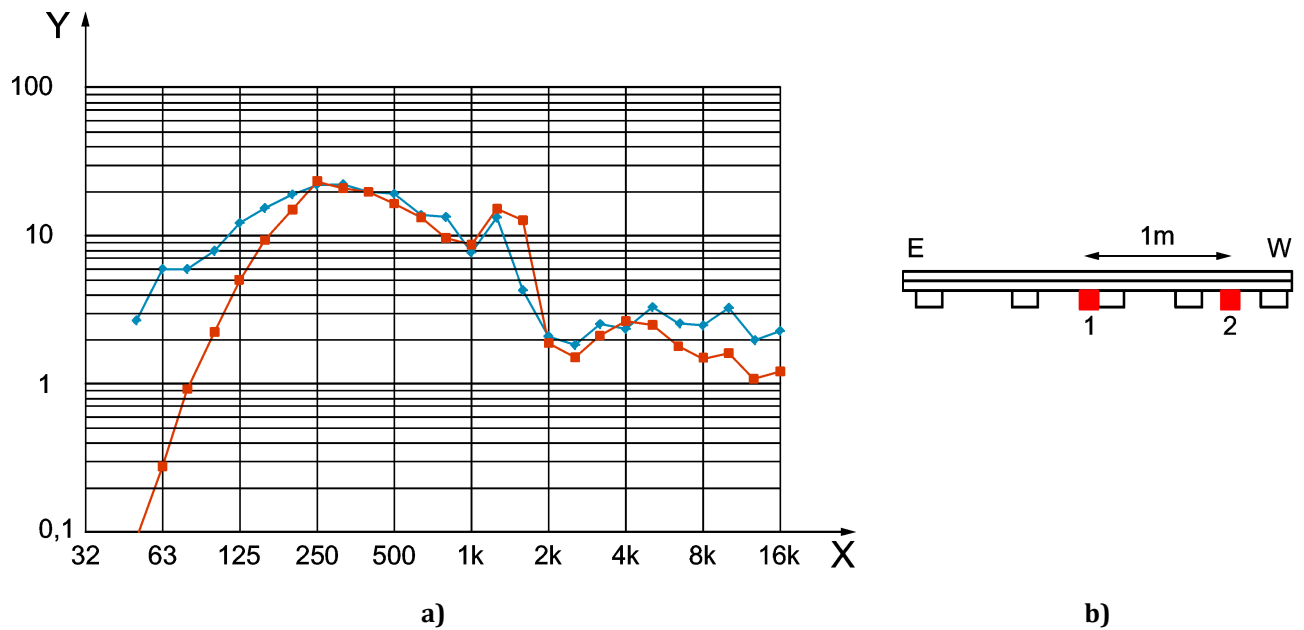
1 accelerometer positioned near a sleeper

2 accelerometer positioned 1 m further along between sleepers

NOTE Pass-by was carried out with a freight train at 80 km/h.

—◆— Acc #1
 —■— Acc #2

Figure B.22 — Vertical track decay rate determined from two different accelerometers along the rail on a Swiss ballasted track with monobloc sleepers



Key

Y track decay rate in dB/m

X frequency in Hz

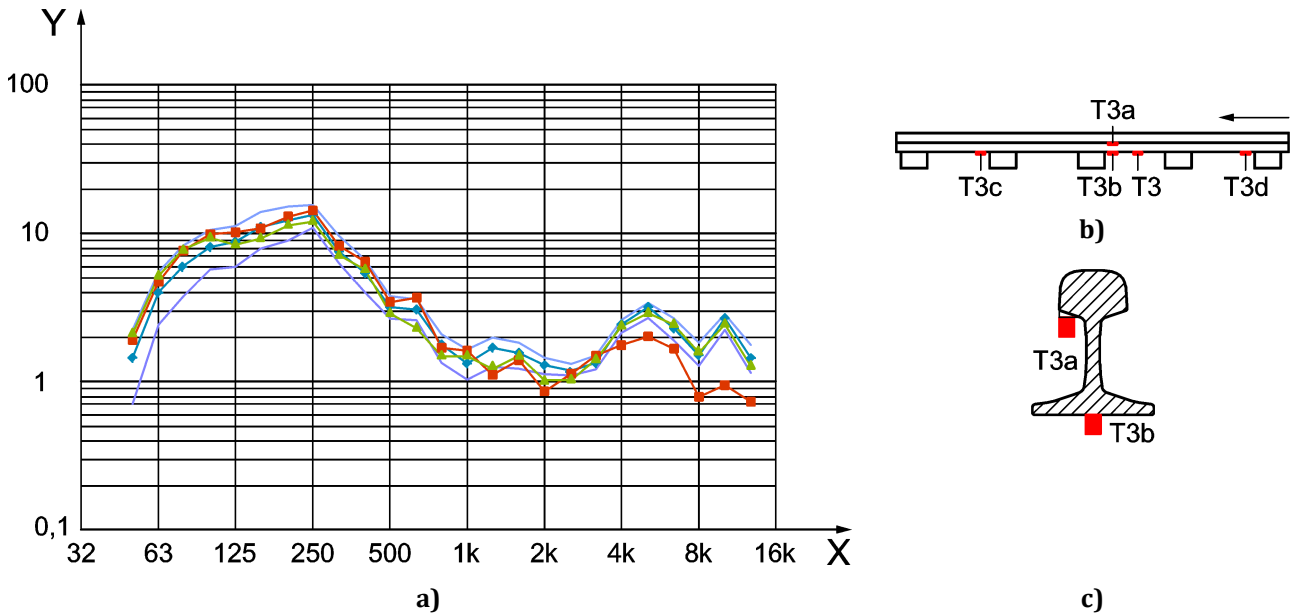
1 accelerometer positioned near a sleeper

2 accelerometer positioned 1 m further along between sleepers

NOTE Results corresponding to a pass-by of a passenger train at 100 km/h.

—◆— Acc #1
 —■— Acc #2

Figure B.23 — Vertical track decay rate determined from two different accelerometers along the rail on a Swiss ballasted track with monobloc sleepers



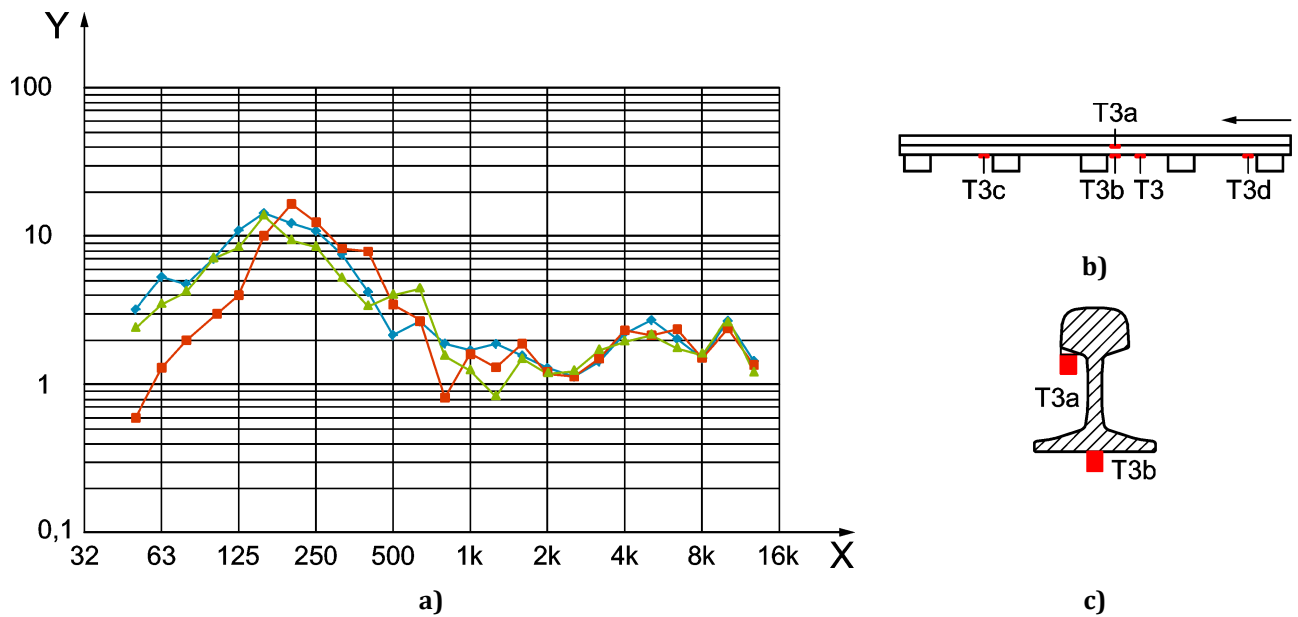
Key

Y	track decay rate in dB/m		T3b - 120 km/h
X	frequency in Hz		Indirect +
	T3 - 120 km/h		Indirect -
	T3a - 120 km/h		

NOTE 1 Results of a pass-by of a mixed test train at 120 km/h.

NOTE 2 The standard deviation curves are indicated with + and -.

Figure B.24 — Vertical track decay rate determined from three different accelerometer positions on a German ballasted track with monobloc sleepers

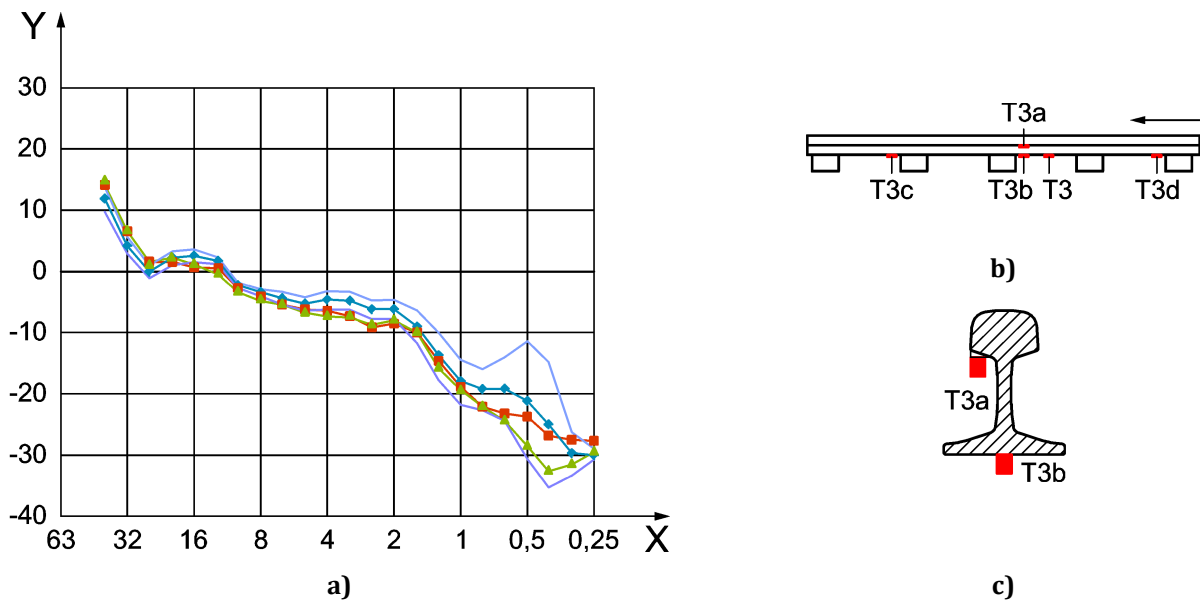


Key

Y	track decay rate in dB/m	—■—	T3c - 80 km/h
X	frequency in Hz	—▲—	T3d - 80 km/h
	T3 - 80 km/h	—◆—	

NOTE Results corresponding to a pass-by of a mixed test train at 80 km/h.

Figure B.25 — Vertical track decay rate determined from three different accelerometer positions along the rail on a German ballasted track with monobloc sleepers



Key

Y	L_R in dB re $1\mu\text{m}$		Average at 80 km/h T3b
X	wavelength in cm		Average at 80 km/h T3+
	Average at 80 km/h T3		Average at 80 km/h T3-
	Average at 80 km/h T3a		

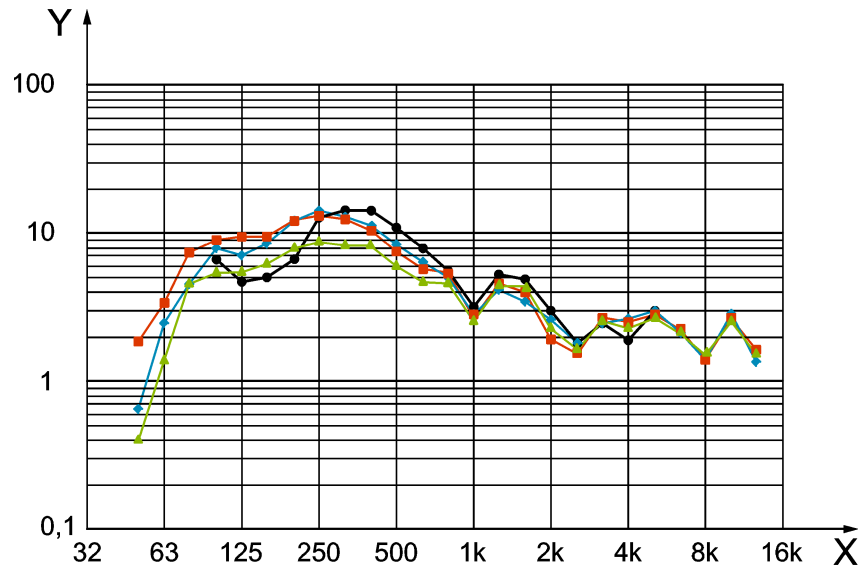
NOTE 1 Results averaged over multiple pass-bys of a mixed test train at 80 km/h

NOTE 2 The standard deviation curves are indicated with + and -.

Figure B.26 — Combined roughness determined with energy method on a German ballasted track with monobloc sleepers

B.8 Effect of speed and averaging

The train speed can affect the track decay rate result due to the amount of energy present in the signal. It is therefore recommended to conduct measurements at more than one speed if possible. Some examples of speed variation are shown for decay rates in Figure B.27, Figure B.28 and Figure B.29, for combined roughness in Figure B.30 and for transfer functions in Figure B.31.

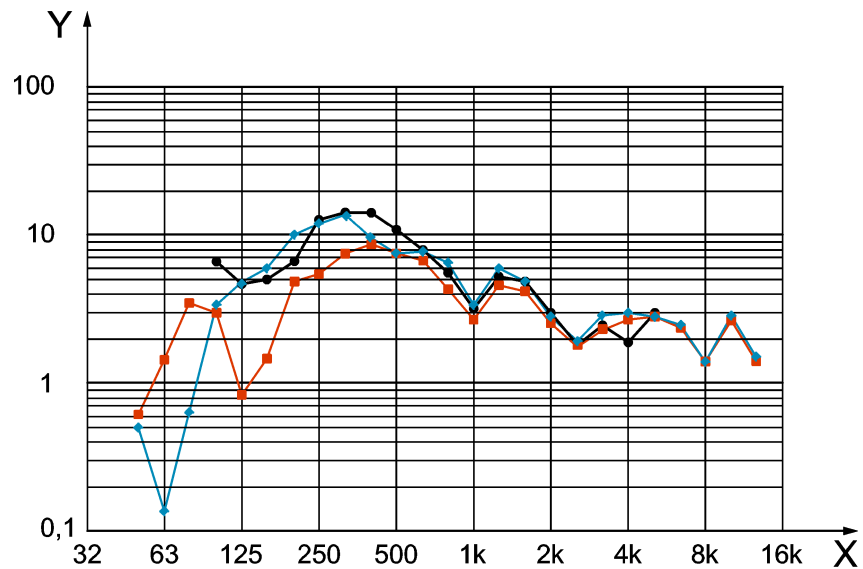


Key

Y	track decay rate in dB/m		160 km/h
X	frequency in Hz		60 km/h
	80 km/h		Direct

NOTE Results corresponding to several pass-bys of one EMU 2 car train at three train speeds and then averaged.

Figure B.27 — Vertical track decay rate determined with the energy method on a German track with monobloc sleepers and ballast

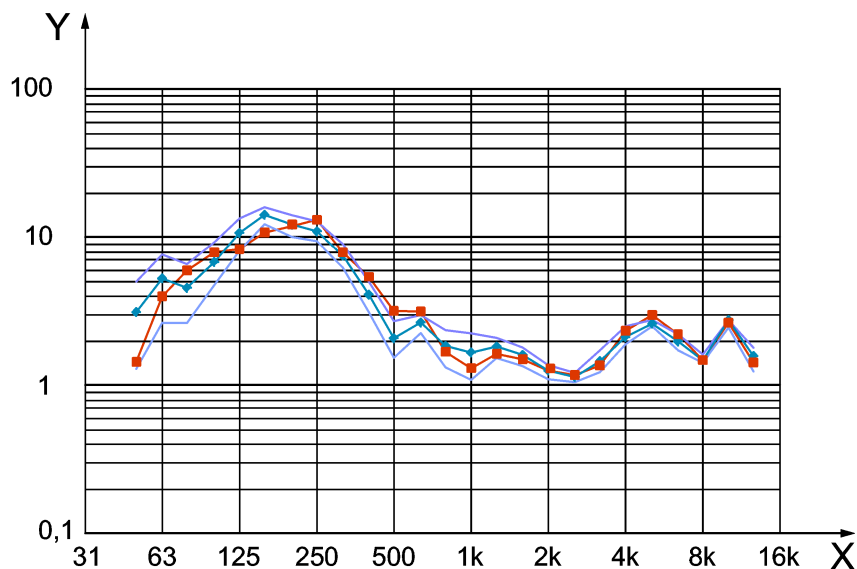


Key





Y	track decay rate in dB/m		160 km/h
X	frequency in Hz		Direct
	80 km/h		

NOTE Several pass-bys of one EMU 4 car train were carried out at two train speeds and then averaged.

Figure B.28 — Vertical track decay rate determined with the energy method on a German track with monobloc sleepers and ballast



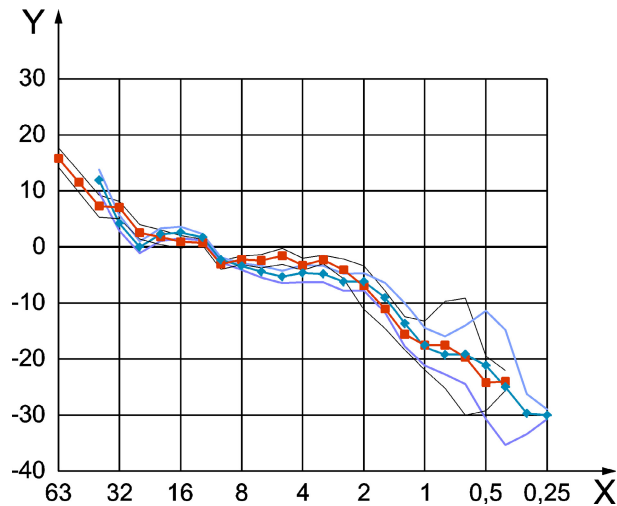
Key

Y	track decay rate in dB/m		T3 - 120 km/h
X	frequency in Hz		Indirect+
	T3 - 80 km/h		Indirect-

NOTE 1 Results corresponding to several pass-bys of a mixed test train at two train speeds and then averaged.

NOTE 2 The standard deviation curves are indicated with + and -.

Figure B.29 — Vertical track decay rate determined with energy method on a German ballasted track with monobloc sleepers



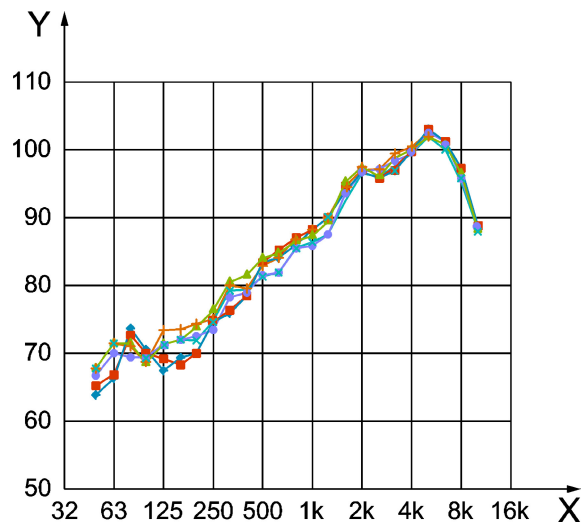
Key

Y	L_R in dB re $1\mu\text{m}$	—	Average at 80 km/h T3+
X	wavelength in cm	—	Average at 80 km/h T3-
—●—	Average at 80 km/h T3	—	Average at 120 km/h T3+
—■—	Average at 120 km/h T3	—	Average at 120 km/h T3-

NOTE 1 Results corresponding to multiple pass-bys of a mixed test train at two train speeds and then averaged.

NOTE 2 The standard deviation curves are indicated with + and -.

Figure B.30 — Combined roughness determined with energy method on a German ballasted track with monobloc sleepers



Key

Y	$L_{Hpr,nl}$ in dB re $20\text{ Pa}/\sqrt{\text{m}}$	—▲—	4-1b120M3
X	frequency in Hz	—●—	3-4b120M3
—●—	3-3b80M3	—+—	4-3b120M3
—■—	4-2b80M3	—x—	3-5b120M3

NOTE Results corresponding to several pass-bys of a mixed test train at two train speeds.

Figure B.31 — Total transfer function determined on a German ballasted track with monobloc sleepers

B.9 Effect of wheel defects

Wheel defects such as flat spots or polygonization can significantly affect the track decay rate analysis, increasing the uncertainty and dominating the average roughness of the whole train. If combined roughness is to be determined, it is preferable to obtain the decay rate estimate from a train without wheel defects and use this when determining the combined roughness.

The significance of wheel flats can be assessed by comparing the peak noise level due to the flat to the peak level of other wheels in the train. If the increase due to the wheel flat exceeds 3 dB it may affect decay rate estimates and combined roughness.

B.10 Effect of temperature

The temperature of the rail pad can affect the track decay rate. If the rail pad temperature changes significantly during a pass-by due to the successive wheel excitation and the material is strongly temperature dependent in the applicable range, then a difference may be found in decay rate at the front and the rear of the pass-by.

Also measurements taken at different times or locations with a significant difference in rail and pad temperature may therefore differ. Therefore, when determining combined roughness using decay rates derived from pass-by data, it is recommended to use a decay rate measured under similar temperature conditions.

B.11 Effect of load

A loaded track will show some difference in decay rate in comparison with unloaded track (see comparison direct and pass-by results). But for loaded track during a pass-by, the relative difference between different axle loads is generally smaller than that with unloaded track. In addition, load will tend to vary along the train.

Annex C (informative)

Slope methods

C.1 Single accelerometer slope method

The time signal of the railhead vibration (single accelerometer) is filtered to obtain level histories $L_a(f_c, t)$ for each one-third octave frequency band in the range 25 Hz to 10 kHz. The time interval of the level history is taken at 1/16 s.

Where clearly detectable and approximately linear in dB/s, the slope is calculated from manually or automatically selected points either in the approach slope, the departure slope, slopes near one or more wheels, or combinations of these.

The decay rate at each one-third octave centre frequency f_c is estimated from

$$D(f_c) = 1/v \cdot dL_a(f_c)/dt \text{ in [dB/m]} \quad (\text{C.1})$$

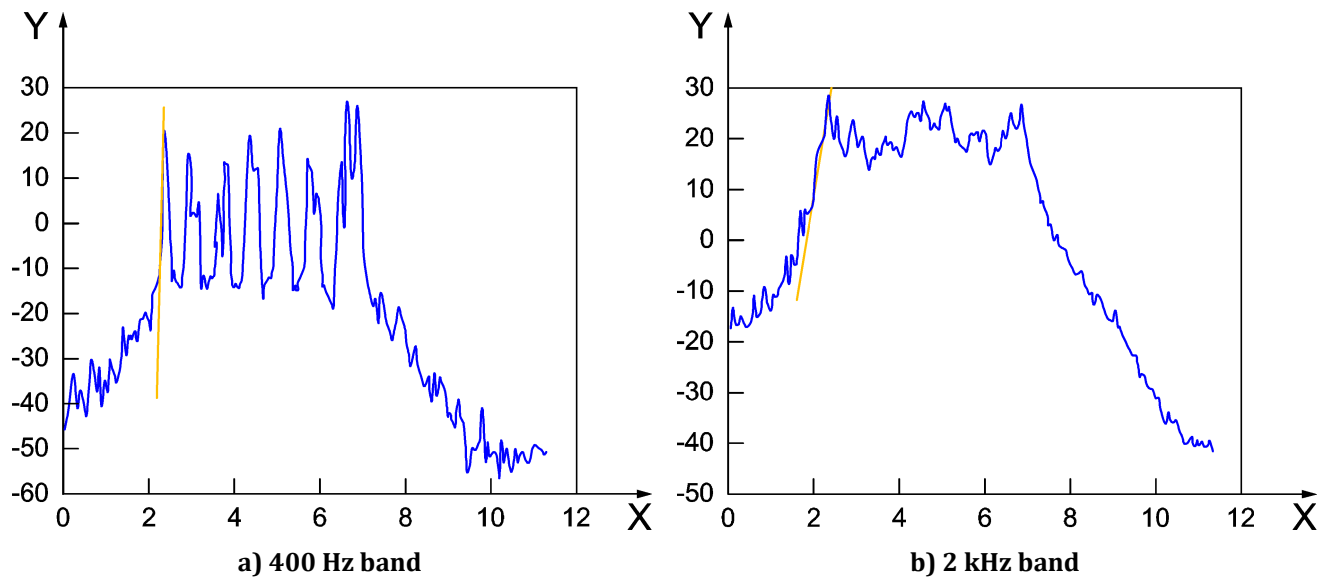
Uncertainty may be reduced by averaging over:

- multiple slopes;
- multiple pass-bys;
- several train speeds;

and by using points with amplitude more than 10 dB apart.

The part of the slope to be considered should be close to the peak of the wheel pass-by. The method can be automated by taking the derivative of the whole level history and averaging the top 85 % values found over the whole pass-by.

For tracks with a low decay rate, the influence of other wheels may affect the result, leading potentially to an underestimation of the decay rate. This may be minimized by using parts of the pass-by curve most distant from other wheels, i.e. the front or rear slope or between widely spaced wheels.



Key

Y $L(t)$ in dB

X t in s

Figure C.1 — Example of manual slope estimation from level history of individual one-third octave bands

C.2 Two accelerometer method

Two accelerometers are placed under the middle of the rail foot close to two successive sleepers. The time signals of the railhead vibration are both filtered to obtain level histories for each one-third octave frequency band in the range 25 Hz to 10 kHz. The time interval of the level history is 1/32 s.

The level difference in dB between the two sensors is determined per frequency band from those spectra in the series when the first wheel is less than 2 m from the first vibration sensor. The decay rate is obtained from the level difference divided by the distance between the two sensors.

Bibliography

- [1] COMMISSION REGULATION (EU) No 1304/2014 of 26 November 2014 on the technical specification for interoperability relating to the subsystem 'Rolling stock — Noise' amending Decision 2008/232/EC and repealing Decision 2011/229/EU
- [2] JANSSENS M.H.A., DITTRICH M.G., DE BEER F.G., JONES C.J.C. Railway noise measurement method for pass-by noise, total effective roughness, transfer functions and track spatial decay. *J. Sound Vibrat.* 2006, **293** pp. 1007–1028
- [3] JANSEN H.W., DITTRICH M.G. User Manual Pass-by Analysis Software, TNO Report (2002)
- [4] DITTRICH M.G. *Track decay rate measurements using the PBA technique*. Euronoise Tampere, Finland, 2006
- [5] JANSEN H.W., JANSSENS M.H.A., DITTRICH M.G. Practical applications of total wheel/rail roughness measurements during train pass-bys, 9th IWRN, Munich, Germany (2007)
- [6] JANSEN H.W., DITTRICH M.G. *Separation of Rolling Noise and Aerodynamic Noise by In-Service Measurement of Combined Roughness and Transfer Functions on a High Speed Slab Track*, 10th IWRN. Nagahama, Japan, 2010
- [7] ENGELS R. Pass-by analysis of vertical track decay rate on several benchmark datasets, TNO report TNO-DV 2012 C022, Internship Report, The Hague (2012)
- [8] ENGELS R. *Indirect measurements of track decay rate and combined roughness by means of pass-by analysis, Internship Report*. DB Systemtechnik, 2012
- [9] THOMPSON D.J., JONES C.J.C. *Study on the sensitivity of the indirect roughness method to variations in track and wheel parameters, STAIRRS report STR23TR030501ISVR1*. ISVR, 2001
- [10] BÜTIKOFER R. sonRAIL Beschleunigungsmessungen: Zur Problematik von Übersteuerungen, Untersuchungsbericht Nr. 445403-1, EMPA, Bern (2007)
- [11] OPPEL M. Indirect Determination of the Track Decay Rate and the Wheel/Rail Roughness from Train Pass-by Rail Accelerations, Thesis for the degree of Master of Science in Engineering (MScEng) / Dipl.-Ing, TU Berlin (2011)
- [12] KEPHALOPOULOS S., PAVIOTTI M., ANFOSSO-LÉDÉE F. Common Noise Assessment Methods in Europe (CNOSSOS-EU) EUR 25379 EN. Luxembourg: Publications Office of the European Union (2012); see
- [13] EN 61260-1, *Electroacoustics — Octave-band and fractional-octave-band filters — Part 1: Specifications (IEC 61260-1)*
- [14] EN ISO 3095, *Acoustics — Railway applications — Measurement of noise emitted by railbound vehicles (ISO 3095)*
- [15] ISO 5348, *Mechanical vibration and shock — Mechanical mounting of accelerometers*

British Standards Institution (BSI)

BSI is the national body responsible for preparing British Standards and other standards-related publications, information and services.

BSI is incorporated by Royal Charter. British Standards and other standardization products are published by BSI Standards Limited.

About us

We bring together business, industry, government, consumers, innovators and others to shape their combined experience and expertise into standards-based solutions.

The knowledge embodied in our standards has been carefully assembled in a dependable format and refined through our open consultation process. Organizations of all sizes and across all sectors choose standards to help them achieve their goals.

Information on standards

We can provide you with the knowledge that your organization needs to succeed. Find out more about British Standards by visiting our website at bsigroup.com/standards or contacting our Customer Services team or Knowledge Centre.

Buying standards

You can buy and download PDF versions of BSI publications, including British and adopted European and international standards, through our website at bsigroup.com/shop, where hard copies can also be purchased.

If you need international and foreign standards from other Standards Development Organizations, hard copies can be ordered from our Customer Services team.

Copyright in BSI publications

All the content in BSI publications, including British Standards, is the property of and copyrighted by BSI or some person or entity that owns copyright in the information used (such as the international standardization bodies) and has formally licensed such information to BSI for commercial publication and use.

Save for the provisions below, you may not transfer, share or disseminate any portion of the standard to any other person. You may not adapt, distribute, commercially exploit, or publicly display the standard or any portion thereof in any manner whatsoever without BSI's prior written consent.

Storing and using standards

Standards purchased in soft copy format:

- A British Standard purchased in soft copy format is licensed to a sole named user for personal or internal company use only.
- The standard may be stored on more than 1 device provided that it is accessible by the sole named user only and that only 1 copy is accessed at any one time.
- A single paper copy may be printed for personal or internal company use only.

Standards purchased in hard copy format:

- A British Standard purchased in hard copy format is for personal or internal company use only.
- It may not be further reproduced – in any format – to create an additional copy. This includes scanning of the document.

If you need more than 1 copy of the document, or if you wish to share the document on an internal network, you can save money by choosing a subscription product (see 'Subscriptions').

Reproducing extracts

For permission to reproduce content from BSI publications contact the BSI Copyright & Licensing team.

Subscriptions

Our range of subscription services are designed to make using standards easier for you. For further information on our subscription products go to bsigroup.com/subscriptions.

With **British Standards Online (BSOL)** you'll have instant access to over 55,000 British and adopted European and international standards from your desktop. It's available 24/7 and is refreshed daily so you'll always be up to date.

You can keep in touch with standards developments and receive substantial discounts on the purchase price of standards, both in single copy and subscription format, by becoming a **BSI Subscribing Member**.

PLUS is an updating service exclusive to BSI Subscribing Members. You will automatically receive the latest hard copy of your standards when they're revised or replaced.

To find out more about becoming a BSI Subscribing Member and the benefits of membership, please visit bsigroup.com/shop.

With a **Multi-User Network Licence (MUNL)** you are able to host standards publications on your intranet. Licences can cover as few or as many users as you wish. With updates supplied as soon as they're available, you can be sure your documentation is current. For further information, email subscriptions@bsigroup.com.

Revisions

Our British Standards and other publications are updated by amendment or revision.

We continually improve the quality of our products and services to benefit your business. If you find an inaccuracy or ambiguity within a British Standard or other BSI publication please inform the Knowledge Centre.

Useful Contacts

Customer Services

Tel: +44 345 086 9001

Email (orders): orders@bsigroup.com

Email (enquiries): cservices@bsigroup.com

Subscriptions

Tel: +44 345 086 9001

Email: subscriptions@bsigroup.com

Knowledge Centre

Tel: +44 20 8996 7004

Email: knowledgecentre@bsigroup.com

Copyright & Licensing

Tel: +44 20 8996 7070

Email: copyright@bsigroup.com

BSI Group Headquarters

389 Chiswick High Road London W4 4AL UK